Svoluji k zapůjčení své diplomové práce ke studijním účelům a prosím, aby byla vedena přesná evidence vypůjčovatelů. Převzaté údaje je vypůjčovatel povinen řádně ocitovat.

Charles University

Faculty of Science

Study programme: Biology

Branch of study: Genetics, Molecular Biology and Virology

Bc. Jana Kráčmarová

Role of MAPK in regulation of cytoplasmic polyadenylation during meiotic maturation of mammalian oocytes

Role MAPK v regulaci cytoplazmatické polyadenylace během meiotického zrání savčích oocytů

DIPLOMA THESIS

Supervisor: Ing. Michal Kubelka, CSc.

Prague, 2017

Prohlašuji, že jsem závěrečnou práci zpracovala samostatně a že jsem uvedla všechny použité informační zdroje a literaturu. Tato práce ani její podstatná část nebyla předložena k získání jiného nebo stejného akademického titulu.

V Praze, 27.4.2017

Jana Kráčmarová

I would like to sincerely thank Michal Kubelka for being my supervisor, investing his time to my training and staying calm when I was stressed out. Special thanks go to Andrej Šusor for creating enthusiastic work environment and coming up with new ideas all the time. Many thanks belong to all members of the Laboratory of Biochemistry and Molecular Biology of Germ Cells, especially to Jarka Šupolíková for keeping the lab clean and having solution to any problem. I am grateful to Edgar del Llano Solanas for his comments and corrections.

The greatest thanks go to my mum, dad and sister for their enormous support and to Vendula Čečmanová and Miroslav Přibyl for long discussions about science, life and how to stay alive when doing science.

This work was supported by the Czech Science Foundation (project no. GA15-22765S).

ABSTRACT

Mammalian oocytes undergoing meiotic maturation are transcriptionally silent and gene expression is therefore regulated at the level of translation. One of the well established mechanisms employed in translational regulation of maternal mRNAs in oocytes is cytoplasmic polyadenylation. This process is generally controlled by phosphorylation and activation of cytoplasmic polyadenylation element binding protein (CPEB). The aim of this thesis is to determine the role of mitogen-activated protein kinase (MAPK) in regulation of CPEB-mediated cytoplasmic polyadenylation in maturing mouse and porcine oocytes. For this purpose, MAPK activity was inhibited using its specific inhibitor, GDC-0994 and the effect of MAPK inhibition on cyclin B1 mRNA polyadenylation was monitored. In mouse oocytes, MAPK inhibition impaired neither cyclin B1 mRNA polyadenylation nor its translation and MAPK is thus unlikely to be involved in regulation of cytoplasmic polyadenylation in this species. Based on the results of experiments performed using porcine oocytes, the possible role of MAPK in CPEB-mediated cytoplasmic polyadenylation can neither be confirmed nor ruled out.

Keywords: cytoplasmic polyadenylation, mouse oocyte, porcine oocyte, mitogen-activated protein kinase (MAPK), cyclin B1, GDC-0994 inhibitor

ABSTRAKT

V průběhu meiotického zrání savčích oocytů neprobíhá transkripce a exprese genů je proto řízena na úrovni translace. Jedním z dobře prozkoumaných mechanismů, které se podílí na regulaci translace maternálních mRNA v oocytech, je cytoplazmatická polyadenylace. Ta je zahájena aktivační fosforylací proteinu, který se váže na cytoplazmatický polyadenylační element (CPEB protein, z ang. *cytoplasmic polyadenylation binding protein*). Cílem této práce je zjistit, jakou roli hraje mitogenem aktivovaná proteinkináza (MAPK) v regulaci cytoplazmatické polyadenylace zprostředkované CPEB proteinem ve zrajících myších a prasečích oocytech. Za tímto účelem byla aktivita MAPK inhibována specifickým inhibitorem (GDC-0994) a byl zkoumán efekt této inhibice na polyadenylaci mRNA pro cyklin B1. V myších oocytech neovlivnila inhibice MAPK ani polyadenylaci, ani translaci mRNA pro cyklin B1, z čehož vyplývá, že se MAPK pravděpodobně nepodílí na regulaci cytoplazmatické polyadenylace v tomto živočišném druhu. Na základě výsledků experimentů provedených na prasečích oocytech nelze vyloučit ani potvrdit případnou úlohu MAPK v regulaci cytoplazmatické polyadenylace.

Klíčová slova: cytoplazmatická polyadenylace, myší oocyt, prasečí oocyt, mitogenem aktivovaná proteinkináza (MAPK), cyklin B1, inhibitor GDC-0994

CONTENTS

ABBREVIATIONS

4E-BP	Eukaryotic translation initiation factor 4E-binding protein
4E-T	Eukaryotic translation initiation factor 4E transporter
AURKA	Aurora kinase A
BSA	Bovine serum albumin
BTG4	B-cell translocation gene-4
CaMKII	Calcium/calmodulin-dependent protein kinase II
Cdk1	Cyclin-dependent kinase 1
CEOs	Cumulus-enclosed oocytes
CPE	Cytoplasmic polyadenylation element
CPEB	Cytoplasmic polyadenylation element-binding protein
CPSF	Cleavage and polyadenylation specificity factor
DMSO	Dimethyl sulfoxide
DOs	Denuded oocytes
eIF2α	Eukaryotic translation initiation factor 2α
eIF4E	Eukaryotic translation initiation factor 4E
eIF4G	Eukaryotic translation initiation factor 4G
ePAB	Embryonic poly(A)-binding protein
ERK	Extracellular signal-regulated kinase
FBS	Fetal bovine serum
FSH	Follicle-stimulating hormone
GAPDH	Glyceraldehyde-3-phosphate dehydrogenase
GV	Germinal vesicle
GVBD	Germinal vesicle breakdown
IBMX	3-isobutyl-1-methylxanthine
IU	International unit
LH	Luteinizing hormone
MI/II	Metaphase I/II
MAPK	Mitogen-activated protein kinase
MBP	Myelin basic protein
MPF	Maturation or M-phase promoting factor

mTOR	Mammalian target of rapamycin
p90/RSK	Ribosomal protein S6 kinase 1
PABP	Poly(A)-binding protein
PAGE	Polyacrylamide gel electrophoresis
PAS	Polyadenylation signal
PAT	Poly(A) tail assay
PB	Polar body
PBS	Phosphate-buffered saline
PMSG	Pregnant mare’s serum gonadotropin
PVA	Polyvinyl alcohol
RINGO	Rapid inducer of G2/M transition in oocytes
SCP	Synaptonemal complex protein
SDS	Sodium dodecyl sulfate
TBE	Tris-borate-EDTA buffer
TM	Transfer medium
TBS	Tris-buffered saline
ZP	Zona pellucida

1. INTRODUCTION

Sexual reproduction of mammals depends on production of gametes, or germ cells, by the process of gametogenesis. Female version of gametogenesis is called oogenesis, while male equivalent is called spermatogenesis. During gametogenesis, a diploid progenitor cell undergoes meiosis which consists of two rounds of cell division and results in generation of haploid germ cells. In males, four equal-sized spermatids are produced from one progenitor cell, whereas in females, a single large haploid ovum is created through asymmetric divisions of a progenitor cell, leaving the excessive maternal chromosomes extruded in two small polar bodies. Moreover, unlike male meiosis, which starts at the onset of puberty and once initiated it proceeds uninterrupted, female meiosis is initiated prenatally and is arrested twice. The first meiotic arrest occurs at the prophase of the first meiotic division and it is not released until the female becomes sexually mature, which takes years in human and weeks in mouse. The second meiotic arrest oocurs at the metaphase of the second meiotic division and it is released after fertilization. Importantly, during the period which starts at the time when the prophase-arrested oocyte resumes meiosis and ends at the time of embryonic genome activation, transcription is turned off. Thus, gene expression is controlled at post-transcriptional level, mainly by regulation of translation, mRNA and protein stability and by post-translational protein modifications .

The research in our laboratory is focused on regulation of translation during meiosis of mammalian oocytes. Both ends of mRNA play role in translation initiation. The 7-methylguanosine cap on the 5' end of mRNA is bound by eukaryotic translation initiation factor 4E (eIF4E) and serves as a basis for translation initiation complex assembly. My colleagues have recently shown that a subset of mRNAs is translated after meiotic resumption of mouse oocytes in the vicinity of the chromosomes and this translation depends on phosphorylation of eukaryotic translation initiation factor 4E-binding protein 1 (4E-BP1) which in its unphosphorylated state binds to eIF4E and prevents formation of the translation initiation complex (Susor *et al*. 2015). They have also shown that 4E-BP1 is the only member of 4E-BP protein family present in maturing mouse oocytes and its phosphorylation is positively regulated by mammalian target of rapamycin (mTOR) kinase and cyclin-dependent kinase 1 (Cdk1) (Jansova *et al*. 2017). The poly(A) tail present on the 3' end of mRNA can also promote translation depending on its length. A group of mRNAs possessing short poly(A) tails is stored in the cytoplasm of prophase-arrested oocytes and is not translated until the poly(A) tail is elongated by the process of cytoplasmic polyadenylation. The mechanisms regulating cytoplasmic polyadenylation have been investigated in our laboratory using porcine oocytes. In particular, it has been shown that Aurora kinase A, which has been previously proposed to

activate cytoplasmic polyadenylation in *Xenopus* oocytes, is not involved in activation of this process in porcine oocytes (Komrskova *et al*. 2014). In my project I aimed to further investigate regulation of cytoplasmic polyadenylation using not only porcine, but also mouse oocytes. It has been demonstrated, that protein synthesis is necessary for release from the prophase arrest of porcine oocytes, whereas mouse oocytes resume meiosis even when the overall protein synthesis is inhibited (Fulka *et al*. 1986). Based on this finding I assume that regulation of cytoplasmic polyadenylation might differ in oocytes of these two species.

The correct progression of meiosis is essential for generation of oocytes capable of giving rise to a new individual after fertilization. A better understanding of molecular mechanisms controlling meiotic division can provide explanation for meiotic abnormalities often occuring in mammalian oocytes.

2. LITERATURE REVIEW

2.1 Mammalian oogenesis

Oogenesis is the process by which the female gamete, or ovum, is created. It consists of three successive stages. During the first stage, or multiplication stage, primordial germ cells migrate from the site of their inception to the genital ridge of developing embryo. The migrating primordial germ cells proliferate and once they reach the final destination they give rise to oogonia which undergo several more rounds of mitosis. This mitotic activity is the major determinant of oocyte pool. The oogonia eventually enter meiosis, progress through leptotene, zygotene and pachytene stages of meiotic prophase I and arrest at the diplotene stage. The nucleus of diplotene-arrested oocyte is called germinal vesicle (GV) and the oogonium which has undergone mitosis-to-meiosis transition is called primary, or GV stage oocyte. The primary oocytes are surrounded by one layer of flat granulosa cells forming a primordial follicle. At the time of birth all oocytes within the female ovary have either reached the primary oocyte stage or undergone atresia (degeneration).

During a female life span, small number of primordial follicles is steadily released from the resting pool. In the absence of follicle-stimulating hormone (FSH) the growing follicles undergo atresia. When a female becomes sexually mature, the hypothalamus-pituitary-ovarian axis is activated, elevated FSH levels rescue the follicle growth and the follicle passes through following developmental stages: from primary stage (oocyte surrounded by one layer of cuboidal granulosa cells) to secondary (oocyte surrounded by several layers of cuboidal granulosa cells), antral (characterized by formation of a fluid-filled cavity, so called antrum) and preovulatory, also known as Graafian (characterized by increase in antrum volume and two distinguishable populations of granulosa cells inside the follicle - those immediately in contact with the oocyte called cumulus granulosa cells and those lining the wall of the follicle called mural granulosa cells) (Fig. 1). In parallel to follicle development, the oocyte inside the follicle undergoes the second stage of oogenesis, the growth stage (Fig. 1). The growing oocyte, still arrested at the diplotene stage, synthesizes and accumulates various cellular components (such as mRNAs, proteins, ribosomes, mitochondria), increases in volume and secretes a protective glycoprotein membrane, the zona pellucida (ZP). At the end of the growth stage, the oocyte becomes fully-grown and transcription decreases to undetectable levels, which correlates with a change in the nuclear distribution of the chromatin.

The meiotically competent, fully-grown oocyte residing in the preovulatory follicle is capable of entering the last stage of oogenesis, the meiotic maturation. However, the meiotic arrest is maintained by the inhibitory environment within the follicle and it is not released until a surge

in luteinizing hormone (LH) produced by the pituitary occurs. The meiosis resumption is accompanied by the rupture of the preovulatory follicle and the release of maturing oocyte, the process called ovulation. Alternatively, the inhibitory effect of the follicle can be overcome by a simple removal of the oocyte from the follicular compartment and culturing the oocyte *in vitro*. When cultured *in vitro* the oocyte resumes meiosis spontaneously.

The meiosis reinitiation is manifested by germinal vesicle breakdown (GVBD) followed by metaphase plate formation (metaphase I stage; MI), first polar body extrusion and formation of second metaphase plate (metaphase II stage; MII). The oocyte remains arrested at the MII stage and the second meiotic division is completed only when the oocyte is fertilized. The progression from GV to MII stage takes about 12 and 44 hours in mouse and porcine oocytes, respectively.

For detailed information on mammalian oogenesis and specific references please refer to Van den Hurk and Zhao (2005) and Desai *et al*. (2013).

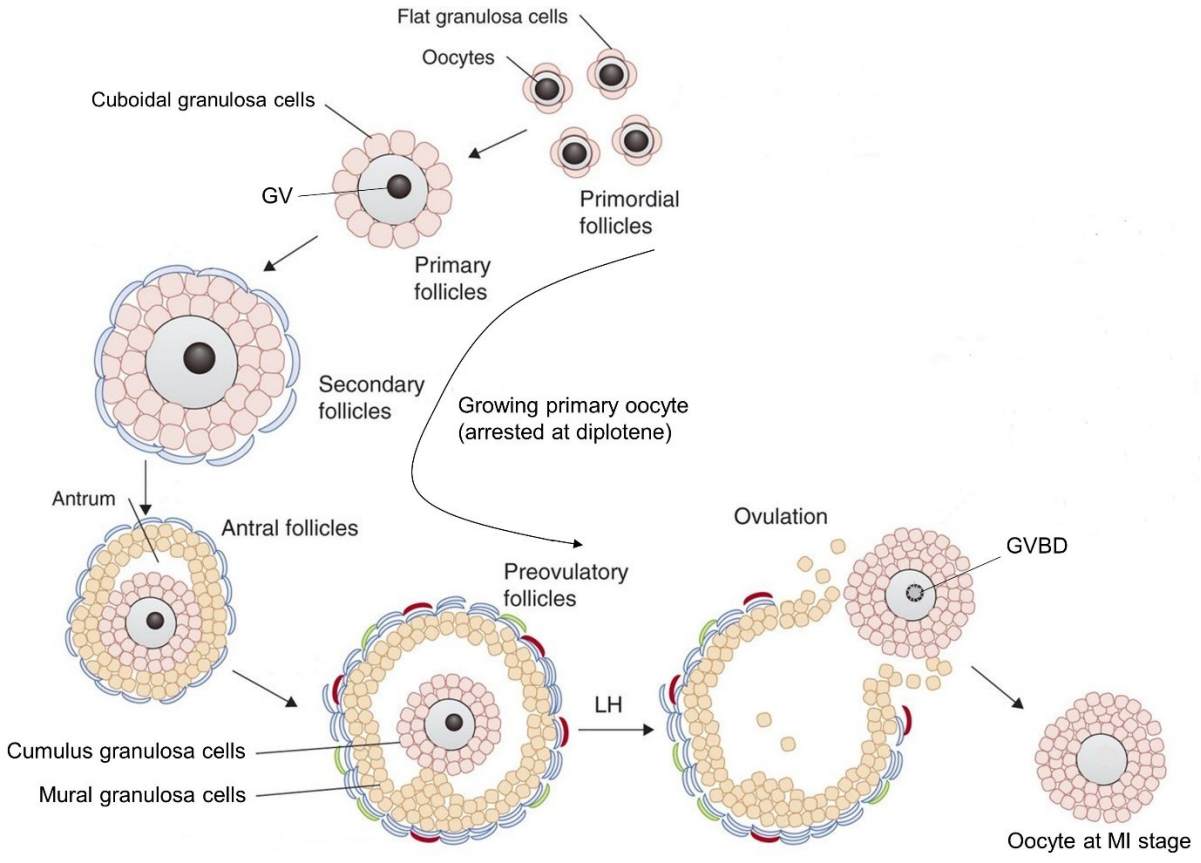

Fig. 1. Mammalian folliculogenesis and oogenesis.

During the growth stage of oogenesis, the diplotene-arrested primary oocyte grows in size and accumulates cellular components, such as mRNAs, proteins and organelles. At the same time, the follicle surrounding the oocyte progresses through several developmental stages starting as primordial follicle and ending up as preovulatory follicle. The fully-grown primary oocyte is released from the preovulatory follicle in response to LH surge and resumes meiosis. Adapted from Georges *et al*. (2014). GV, germinal vesicle; GVBD, germinal vesicle breakdown; LH, luteinizing hormone; MI, metaphase I.

2.2 Molecular control of meiotic maturation

The control of meiotic maturation is very complex and is based on integration of signals from many different signaling pathways. Two key regulators of oocyte meiosis progression, maturation promoting factor and Mos/MEK/MAPK pathway, will be discussed in the following section.

2.2.1 Maturation promoting factor

Maturation or M-phase promoting factor (MPF) is a cytoplasmic factor able to induce entry into M phase (both mitotic and meiotic) in eukaryotic cells. It was first demonstrated by Masui and Markert (1971) who observed that injection of cytoplasm from maturing frog oocytes into immature oocytes induces maturation of recipient oocytes. Roughly twenty years later, two subunits of MPF were identified - a catalytic subunit, cyclin-dependent kinase 1 (Cdk1) and a regulatory subunit, cyclin B (reviewed in Nurse (1990)). Recently, a new component of MPF has been discovered - a kinase called Greatwall. Greatwall kinase inactivates a phosphatase that would otherwise dephosphorylate Cdk1 substrates (Hara *et al*. 2012).

Cdk1 is a serine/threonine protein kinase phosphorylating many substrates which play role in diverse aspects of meiotic maturation such as nuclear envelope breakdown (Adhikari *et al*. 2012) and meiotic spindle formation (Davydenko *et al*. 2013, Jansova *et al*. 2017). Histone H1 is phosphorylated by Cdk1 at several residues and is often used as substrate when assaying Cdk1 activity *in vitro* (Langan *et al*. 1989).

Cdk1 kinase activity is undetectable in GV-arrested oocytes, starts to increase progressively at the time of GVBD and reaches its maximum at MI stage. Then it drops dramatically at the time of the first polar body extrusion and then increases again when the second meiotic spindle is being formed (Fig. 2) (mouse oocytes: Kubiak *et al*. 1992, Verlhac *et al*. 1994; porcine oocytes: Ye *et al*. 2003).

The activity of Cdk1 is controlled by two different mechanisms. First, the association with cyclin B is required for the activation of Cdk1. In porcine GV-arrested oocytes the protein level of cyclin B is very low (Kume *et* al. 2007, Yang *et* al. 2012, Komrskova *et al*. 2014), whereas the amount of cyclin B is in excess to that of Cdk1 in mouse GV-arrested oocytes (Kanatsu-Shinohara *et al*. 2000). This difference in cyclin B amounts could possibly explain why proteosynthesis is required for the meiotic resumption (manifested as GVBD) of porcine, but not mouse oocytes (Fulka *et al*. 1986). Although mouse oocytes undergo GVBD in the absence of proteosynthesis, a nascent synthesis and accumulation of cyclin B is necessary for correct meiotic spinde assembly at the MI stage (i.e. in the absence of proteosynthesis mouse oocytes undergo GVBD but fail to assemble meiotic spindle, whereas porcine oocytes remain arrested

at the GV stage and do not resume meiosis at all) (Gavin *et al*. 1994, Hampl and Eppig 1995b). Moreover, the drop in Cdk1 activity, necessary for and occuring concomitantly with the first polar body extrusion, is caused by partial cyclin B degradation (Hampl and Eppig 1995a). Second, Cdk1 is inactive when phosphorylated at Thr14 and Tyr15 residues. In mouse GV-arrested oocytes, the inhibitory phosphorylation of these two residues is carried out by Wee1B and Myt1 protein kinases (Oh *et al*. 2010), whereas in porcine oocytes, Wee1B but not Myt1 has been shown to be important for the meiotic arrest (Shimaoka *et al*. 2009). After a preovulatory LH surge, Cdc25b phosphatase dephosphorylates and activates Cdk1 in mouse oocytes (Lincoln *et al*. 2002). The identity of phosphatase responsible for Cdk1 activation in maturing porcine oocytes has not been investigated, however, also in this case it has to be a dual target (Thr14 and Tyr15) phosphatase, most likely a porcine homologue of Cdc25b.

2.2.2 Mos/MEK/MAPK pathway

Mitogen-activated protein kinase (MAPK) family consists of three groups of protein kinases: the extracellular signal-regulated kinase (ERK) family, the p38 kinase family, and the c-Jun N-terminal kinase family. This thesis is focused on a potential role of two members of the first group, ERK1 and ERK2, in meiotic maturation of mammalian oocytes.

ERK1 (also termed MAPK3) and ERK2 (also termed MAPK1) are cytoplasmic kinases with high sequence identity and sharing all known substrates, which makes them functionally redundant (Roskoski 2012). For this reason, they will be referred to simply as MAPK in the text of this thesis.

MAPK is active only when phosphorylated at two specific residues by its upstream kinase MEK which is a dual-specificity protein kinase with MAPK being its only known substrate (Roskoski 2012). For this reason, inhibitors targeting MEK activity, such as U0126, are often used to study MAPK function. In somatic cells, MEK is activated by Raf kinase in response to signaling triggered by extracellular growth factors (Roskoski 2012). Interestingly, this is not the case in oocytes, where Mos kinase, rather then Raf kinase, phosphorylates and activates MEK (Verlhac *et al*. 1996). Mos is a serine/threonine kinase expressed exclusivelly in oocytes undergoing meiotic maturation. Mos is absent in GV-arrested oocytes and is synthesized after meiotic resumption in cytoplasmic polyadenylation-dependent manner (Gebauer *et* al. 1994, Verlhac *et al*. 1996, Dai *et al*. 2005). Apart from activating its downstream kinase MEK, Mos promotes MAPK activation also by inhibitory phosphorylation of an unknown phosphatase which would otherwise dephosphorylate and inactivate MAPK (Verlhac *et al*. 2000).

In mouse oocytes, MAPK is activated about two hours after meiotic resumption and remains active throughout the maturation period until the second meiotic arrest at MII stage (Fig. 2) (Verlhac *et al*. 1993). The precise timing of MAPK activation in porcine oocytes is difficult to examine due to not entirely synchronous meiotic resumption of porcine oocytes in maturation culture. MAPK activation has been reported to occur either at the time of GVBD (Inoue *et al.* 1995) or shortly after GVBD (Lee *et al.* 2000, Ellederova *et al*. 2008).

Mos/MEK/MAPK signaling cascade has at least three functions in promoting meiotic maturation. First, MAPK activity in cumulus cells surrounding the oocyte is essential for LH-induced meiotic resumption *in vivo* (Fan and Sun 2004). Second, MAPK is involved in meiotic spindle assembly and stability (Verlhac *et al*. 1993, 1994, 1996, Lefebvre *et* al. 2002, Terret *et al*. 2003). Third, MAPK is important part of cytostatic factor, which causes the oocytes to arrest at the MII stage until fertilization. The oocytes isolated from mutant *mos*$^{-/-}$ mice progress through meiotic maturation but fail to arrest at the MII stage and extrude the second polar body (Verlhac *et al.* 1996). MAPK mediates its functions by phosphorylation of wide range of substrates. For the purpose of this thesis, phosphorylation of two MAPK substrates, myelin basic protein (MBP; Erickson *et al*. 1990) and ribosomal protein S6 kinase (p90/RSK; Dalby *et al.* 1998), has been monitored as marker of MAPK activity.

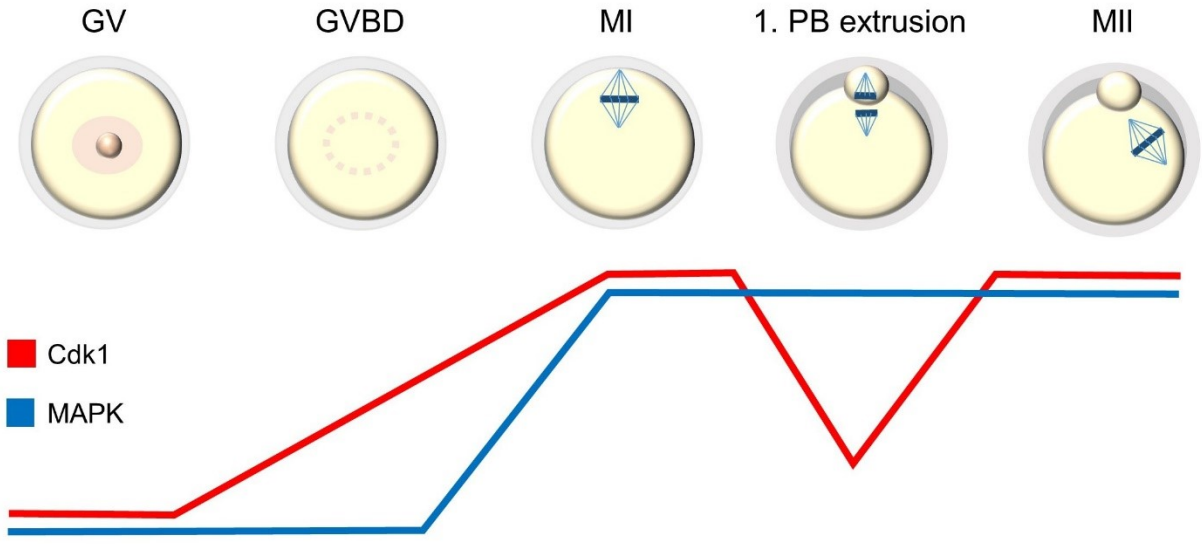

Fig. 2. Cdk1 and MAPK activities during meiotic maturation of mouse oocytes.

Cdk1 activity increases progressively starting at the time of GVBD and reaching its maximum at MI stage, drops at the time of the first polar body extrusion and then increases again and remains high during the MII stage arrest. MAPK is activated after GVBD and remains active throughout the meiotic maturation period. Cdk1 activity appears as a red line and MAPK as a blue line. Cdk1, cyclin-dependent kinase 1; GV; germinal vesicle; GVBD, germinal vesicle breakdown; MI/II, metaphase I/II; MAPK, mitogen-activated protein kinase; PB, polar body.

2.3 Regulation of gene expression during meiotic maturation of mammalian oocytes

During meiotic maturation and early embryonic development, transcription is turned off. All mRNAs encoding proteins important for this period are synthesized during the growth phase of oogenesis and subsequently stored in the cytoplasm until the right time for their translation comes. These mRNAs are termed “dormant”. Several mechanisms of dormant mRNA translation regulation have been proposed, among which cytoplasmic polyadenylation is the most established and considered the primary one. The key player in this mechanism is cytoplasmic polyadenylation element-binding protein (CPEB) which binds to cytoplasmic polyadenylation element (CPE) in 3’UTR of dormant mRNAs. CPEB mediates both repression and subsequent activation of translation.

Newly transcribed mRNA is typically capped at the 5’ end and cleaved and polyadenylated at the 3’ end. Such modified mRNA is exported from the nucleus to the cytoplasm, where the cap is bound by eIF4E and the poly(A) tail is bound by cytoplasmic poly(A)-binding proteins (PABPs). Both eIF4E and PABP interact also with eukaryotic translation initiation factor 4G (eIF4G) creating a protein bridge between the two transcript ends. The pseudo-circularized structure of a transcript promotes translation at least in two ways. First, it enhances the affinity of eIF4E for the cap and as such the formation of the translation initiation complex. Second, it enables the ribosome recycling when a translation run is finished. The circularization of mRNA hence provides a mechanism by which the poly(A) tail regulates translation initiation as the circularization is possible only when the mRNA is polyadenylated. For detailed information on the interplay between the 5’ and 3’ mRNA end I recommend to read the recent review article written by Rissland (2017).

When a CPE-containing mRNA is synthesized it is initially processed in a standard way, i.e. it is capped and polyadenylated. Still in the nucleus the CPE is bound by CPEB and the protein-mRNA complex is then transported to the cytoplasm, where CPEB mediates translational repression by, among others, regulated shortening of the poly(A) tail. Following CPEB phosphorylation, the poly(A) tail is elongated again resulting in activation of mRNA translation (Fig. 3). For detailed information regarding this process refer to sections 2.3.3 and 2.3.4.

Chen *et al*. (2011) employed the polysome mRNA profiling approach to conduct a genome-wide analysis of translation in maturing mouse oocytes. According to this study, there are approximately 7,600 transcripts translated in maturing oocytes as examined by their association with polysomes. About 17% of the identified transcripts increase at least twofold in the polysome fraction as the maturation progresses, implying that their translation was

repressed at the beginning of maturation and subsequently activated. Moreover, 3'UTRs of all identified transcripts were scanned for the presence of several sequence motifs. Notably, CPE was found to be the most abundant motif enriched at least fivefold in the activated transcripts. These results suggest that CPE-mediated translational control plays important role in driving oocyte meiotic maturation.

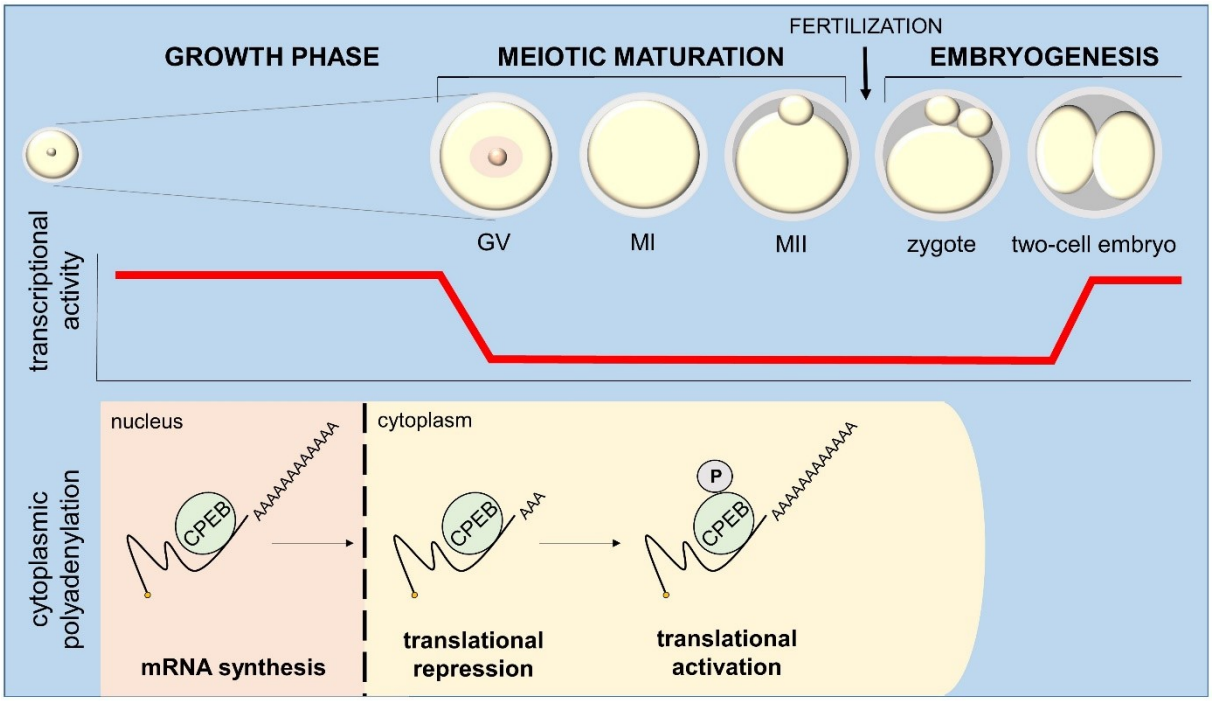

Fig. 3. CPEB-mediated regulation of translation in maturing mammalian oocytes.

During the growth phase of oogenesis, transcription is turned on and the oocyte synthesizes and accumulates dormant mRNAs. When a CPE-containing mRNA is synthesized in the nucleus, its 5' end is capped, 3' end is polyadenylated, CPE is bound by CPEB and the mRNA is exported to the cytoplasm. In the cytoplasm, CPEB mediates shortening of the poly(A) tail and the mRNA is stored in translationally repressed state. When phosphorylated, CPEB mediates elongation of the poly(A) tail and the polyadenylated mRNA is recruited to polysome and translated. CPEB, cytoplasmic polyadenylation element-binding protein; GV, germinal vesicle; GVBD, germinal vesicle breakdown; MI/II, metaphase I/II; P, phospho.

2.3.1 *Cis*-regulatory elements essential for cytoplasmic polyadenylation

There are two essential 3'UTR-residing elements required for mRNA to become translationally repressed right after its synthesis and activated by cytoplasmic polyadenylation either during meiotic maturation or after fertilization. These elements are hexanucleotide polyadenylation signal and cytoplasmic polyadenylation element (Fox *et al*. 1989).

The hexanucleotide polyadenylation signal (PAS; AAUAAA or AUUAAA) is present in nearly all native mRNAs and its primary function is to confer nuclear pre-mRNA cleavage and polyadenylation. Once transcribed, PAS is recognized by cleavage and polyadenylation specificity factor (CPSF) which governs, in cooperation with other proteins, cleavage of the pre-mRNA approximatelly 15-30 nucleotides downstream of the PAS. After cleavage, the poly(A) tail is added by a nuclear poly(A) polymerase (information on nuclear cleavage and polyadenylation of pre-mRNA is reviewed in Charlesworth *et al*. (2013)). Apart from its nuclear function, PAS is also essential for cytoplasmic polyadenylation of dormant mRNAs by recruiting cytoplasmic form of CPSF which in turn recruits cytoplasmic poly(A) polymerase to the 3'end of the mRNA (Dickson *et al*. 1999, Mendez *et al*. 2000b).

The cytoplasmic polyadenylation element (CPE) was first described in certain mRNAs which had been known to be recruited to polysomes in maturing but not immature *Xenopus* oocytes. Truncated versions of this mRNA were synthesized *in vitro*, injected into the cytoplasm of oocyte and assessed for the presence of poly(A) tail at the end of maturation. By this approach, a short U-rich sequence necessary for maturation-dependent polyadenylation was identified and later termed CPE (Fox *et al*. 1989). Moreover, insertion of this U-rich sequence into SV40 RNA which encodes SV40 virion protein and which is not polyadenylated when injected into the oocyte, resulted in polyadenylation of this RNA in maturing *Xenopus* oocytes (McGrew *et al*. 1989). The role of CPE in regulation of dormant mRNA translation was later confirmed also in mouse ooctyes (Huarte *et al*. 1992).

However, the CPE-mediated translational regulation is much more complicated, as the number of CPEs within 3'UTR, their relative position, their distance from the PAS and the presence of other *cis* elements modulate translation of dormant mRNAs. Piqué *et al*. (2008) examined the 3'UTRs of cyclin B1-B5 mRNAs for their ability to confer translational repression and subsequent induction of cytoplasmic polyadenylation when attached to luciferase coding sequence. The 3'UTRs of these mRNAs differ in the number and position of canonical and non-canonical CPEs, as well as of Pumilio-binding element, which is another *cis*-acting element involved in translational regulation. Using a combination of mutagenesis and bioinformatics approach a code describing the relationship between the 3'UTR organization and both extent of translational repression and timing of cytoplasmic polyadenylation in

Xenopus oocytes has been derived. For example, it has been shown that the shorter is the distance between CPE and PAS, the more efficient induction of translation occurrs. On the contrary, no such correlation has been observed in mouse oocytes (Chen *et al*. 2011), suggesting that other mechanisms are involved in fine-tuning of post-transcriptional regulation of gene expression in mouse oocytes.

2.3.2 CPEB proteins

In 1994 a 62 kDa RNA-binding protein specifically recognizing CPE was isolated from *Xenopus* oocyte protein extract and was named cytoplasmic polyadenylation element-binding protein (CPEB) (Hake and Richter 1994). It is composed of the N-terminal region which does not contain any known functional motif and the C-terminal region containing two RNA-recognition motifs and zinc-finger domain. Both RNA-recognition motifs and zinc-finger domain are necessary for RNA binding (Hake *et al*. 1998). Moreover, CPEB has been shown to be indispensable for cytoplasmic polyadenylation of CPE-containing mRNAs, since immunodepletion of this protein from oocyte extract results in the complete loss of polyadenylation activity, which can be restored by addition of exogenous CPEB (Hake and Richter 1994).

Proteins homologous to *Xenopus* CPEB were found in *Drosophila* (Lantz *et al*. 1992), *C. elegans* (Wilson *et al*. 1994), mouse (Gebauer and Richter 1996), cattle (Uzbekova *et al*. 2008), pig (Nishimura *et al*. 2010) and human (Welk *et al*. 2001). In all these species, CPEB is predominantly expressed in oocytes and the C-terminal region possessing RNA-binding activity is highly conserved.

To investigate the function of CPEB protein at the whole-oragnism level, CPEB knockout (KO) mice have been generated by disruption of *cpeb* gene using homologous recombination approach (Tay and Richter 2001). Female KO mice were sterile with severe gonadal defects and oocytes arrested at the pachytene stage. The pachytene arrest was caused by impaired formation of the synaptonemal complex. Two key components of the synaptonemal complex, synaptonemal complex proteins 1 and 3 (SCP1 and 3) are encoded by CPE-containing mRNAs. Notably, only 5% of *scp1* and *scp3* transcripts were associated with polysomes in ovaries of KO mice (compare with 50% in wild-type animals) and the length of their poly(A) tails was markedly reduced. These results suggest that CPEB-mediated polyadenylation occurs and is essential for early stage of mouse oocyte meiosis. To elucidate the function of CPEB after pachytene stage, transgenic mice expressing cpeb mRNA-targeting shRNA under the control of Zona pellucida 3 (*Zp3*) promoter were generated (Racki and Richter 2006). *Zp3* promoter induced oocyte-specific expression at the end of prophase I and so the pachytene

arrest of CPEB KO oocytes was overcome. The CPEB knockdown did not only affect the oocyte itself (parthenogenetic oocyte division, spindle and nuclear abnormalities), but impaired also folliculogenesis as many follicles contained apoptotic granulosa cells.

The vertebrate CPEB protein family actually consists of four CPEB members - CPEB1 (in this thesis referred to as CPEB) and CPEB2-4. CPEB4 has been demonstrated to promote cytoplasmic polyadenylation of some mRNAs during the MI - MII transition of *Xenopus* oocytes (Idea and Méndez 2010), which, however, does not seem to be the case in mouse oocytes (Chen *et al*. 2011). No function of CPEB2 and CPEB3 in meiotic division has been proposed so far. For information on CPEB proteins function in processes other than meiosis refer to Ivshina *et al*. (2014). A recent article (not included in the recommended review) reports that CPEB proteins, with exception of CPEB3, drive mitotic cell cycle progression by promoting sequential polyadenylation and translational activation of CPE-containing mRNAs (Giangarra *et al*. 2015).

2.3.3 Mechanism of CPEB-mediated translational repression

Two models of CPEB-mediated repression of translation have been described so far. The first is based on prevention of eIF4E-eIF4G interaction which is crucial for the assembly of translation initiation complex. The second is based on poly(A) tail shortening which leads to disruption of the circularized mRNA structure. Both models are based on studies conducted in *Xenopus* oocytes.

Model based on prevention of eIF4E-eIF4G interaction

In this model, CPEB protein bound to CPE-containing mRNA interacts with another protein which in turn competes with eIF4G for binding to eIF4E. The first protein proposed to function in this manner is called Maskin. Maskin has been shown to interact with both CPEB and eIF4E (Stebbins-Boaz *et al*. 1999) and to prevent the translation of cyclin B1 mRNA in *Xenopus* oocytes (Cao and Richter 2002) (Fig. 4). However, this model is controversial as the interaction between Maskin and eIF4E is actually very weak (Stebbins-Boaz *et al*. 1999) if any (Minshall *et al*. 2007), likely due to a weak eIF4E-binding motif contained in Maskin (Stebbins-Boaz *et al*. 1999). Moreover, the mouse homologue of Maskin, transforming acidic coiled-coil containing protein 3, lacks the eIF4E-binding motif (Hao *et al*. 2002) making this model unlikely to work in mammalian oocytes.

However, there is another protein that might work in the manner proposed for Maskin. The protein called eIF4E transporter (4E-T) has been shown to be part of a ribonucleoprotein complex together with CPEB, CPE-containing cyclin B1 mRNA and eIF4E1b, a close

homologue of the canonical eIF4E, which, however, does not interact with eIF4G and so cannot promote translation initiation. Although the interaction between eIF4E1b and the 5' cap is weak, it has been suggested that once tethered to the 3'UTR through the eIF4E1b-4E-T-CPEB interaction, it could bind the cap more efficiently and outcompete the canonical eIF4E (Minshall *et al*. 2007). Notably, the homologues of both eIF4E1b (Evsikov *et al*. 2006) and 4E-T (Villaescusa *et al*. 2006) are expressed in mouse oocytes.

Model based on poly(A) tail shortening

The second model of CPEB-mediated translational repression is based on the interaction of mRNA-bound CPEB with both cytoplasmic poly(A) RNA polymerase Gld-2 and poly(A)-specific ribonuclease PARN. Both enzymes are catalytically active, but robust PARN activity keeps the poly(A) tail short (Kim and Richter 2006) (Fig. 4). This model is not mutually exclusive with the first one making it possible that both models work synergistically to repress translation of CPEB-bound mRNAs.

2.3.4 Mechanism of CPEB-mediated translational activation

As well as the mechanism of translational repression, the mechanism of CPEB-mediated translational activation is unclear. In the model where Maskin is employed as the translational repressor and PARN as the factor responsible for the short poly(A), the proposed mechanism of translational activation is as follows: The activating phosphorylation of CPEB causes PARN to be expelled from the ribonucleoprotein complex, which allows Gld2 to elongate poly(A). The poly(A) tail is then bound by embryonic polyadenylate-binding proteins (ePABs) which protect poly(A) tail from degradation. Moreover, ePAB associates with eIF4G causing Maskin displacement and enabling subsequent eIF4G-eIF4E interaction, thereby initiating translation (Cao and Richter 2002, Kim and Richter 2006, Kim and Richter 2007) (Fig. 4).

Whatever the precise mechanism behind translational activation of CPE-containing mRNAs is, it is well established that CPEB phosphorylation on Ser174 residue is important for subsequent cytoplasmic polyadenylation of CPEB-bound mRNAs in *Xenopus* (Mendez *et al*. 2000b, Charlesworth *et al*. 2004), mouse (corresponding residue Thr171; Hodgman *et al*. 2001) and porcine (corresponding residue Thr172; Nishimura *et al*. 2010) oocytes. Yet, there is no general agreement as to the identity of the kinase responsible for CPEB phosphorylation.

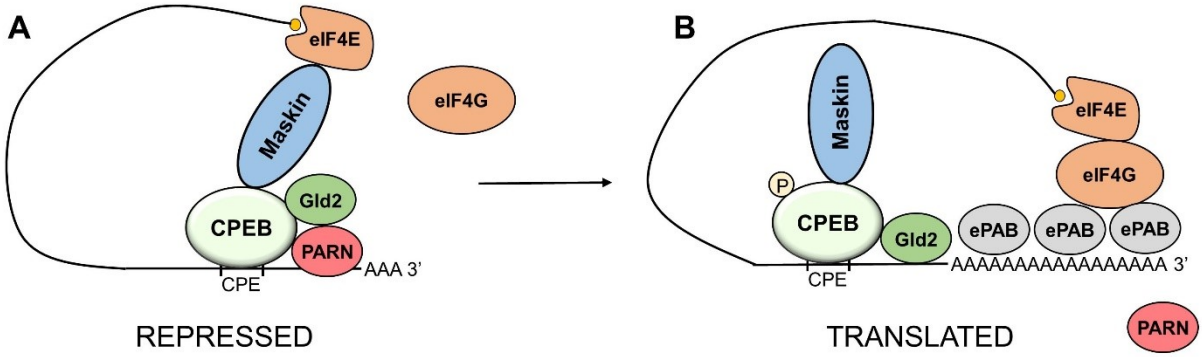

Fig. 4. Maskin-mediated translational repression and activation of CPE-containing mRNAs.

A: Translational repression. CPEB bound to CPE interacts with Maskin which in turn prevents eIF4E-eIF4G interaction. The balance between the opposing effects of Gld2 polymerase and PARN ribonuclease keeps the poly(A) tail short. **B**: Translational activation. CPEB phosphorylation results in PARN expulsion and disruption of Maskin-eIF4E interaction. Gld2 polyadenylates the mRNA and the poly(A) tail is bound by ePAB proteins which aid eIF4E-eIF4G interaction.

Aurora kinase A (AURKA) has been previously proposed to be the CPEB-activating kinase in *Xenopus* (Mendez *et al*. 2000a), mouse (Hodgman *et al*. 2001) and also porcine (Nishimura *et al*. 2010) oocytes. However, this role of AURKA has been questioned by several lines of evidence in all mentioned species. The active form of AURKA was not detected in *Xenopus* oocyte extracts collected 3 hours after meiosis induction, yet CPEB had already been phosphorylated at that time (Keady *et al*. 2007). Moreover, the *Xenopus* oocyte extract retained the ability to phosphorylate CPEB in *in vitro* kinase assay despite either AURKA immunodepletion or inhibition (Keady *et al*. 2007). In mouse oocytes, AURKA inhibition did not prevent B-cell translocation gene-4 (BTG4) protein synthesis which is known to depend on cytoplasmic polyadenylation of btg4 mRNA (Yu *et al*. 2016). A peptide derived from the porcine CPEB sequence encompassing Thr172 was phosphorylated in *in vitro* kinase assay despite the presence of AURKA inhibitor MLN8237. Moreover, the CPEB peptide was not phosphorylated by active recombinant AURKA (Komrskova *et al*. 2014). Altogether, these results strongly suggest that AURKA is not involved in the activating phosphorylation of CPEB.

Kuo *et* al. (2011) has proposed that Cdk1 activated by association with rapid inducer of G2/M transition in oocytes (RINGO) phosphorylates CPEB in *Xenopus* oocytes shortly after meiosis induction and in this way induces cytoplasmic polyadenylation of CPEB-bound mRNAs. However, there are several reasons why this scenario seems implausible. First, no direct evidence has been presented so far. The inhibition of Cdk1/RINGO activity in the oocyte extract used for *in vitro* kinase assay indeed resulted in decreased CPEB phosphorylation, yet it does not prove that Cdk1 directly phosphorylates CPEB (Kuo *et al*. 2011). More importantly, Cdk1 is not active at the time when CPEB is phosphorylated, as examined by the absence of

phosphorylation of histone H1, well established substrate of Cdk1 (Kuo *et al*. 2011). Second, CPEB contains several Cdk1 phosphorylation sites, yet none of them is Ser174 (Mendez *et al*. 2002). As mentioned above, the phosphorylation of CPEB on Ser174 is necessary for induction of CPEB-mediated cytoplasmic polyadenylation (Mendez *et al*. 2000a, Charlesworth *et al*. 2004). Third, CPEB is indeed phosphorylated on six serine residues by Cdk1 at later stage of meiotic progression (at metapahse I), but this phosphorylation targets CPEB for proteasome-mediated degradation (Mendez *et al*. 2002). It has not been explained how a precocious degradation of CPEB would be prevented if Cdk1 phosphorylated CPEB in the early stage of meiotic maturation. Fourth, treatment with roscovitin, an inhibitor of Cdk1 activity, does not prevent early CPEB phosphorylation (Keady *et al*. 2007).

In summary, neither AURKA nor Cdk1 are likely to be responsible for the activating CPEB phosphorylation in *Xenopus* oocytes. Nevertheless, one more candidate has been proposed by Keady *et al*. (2007), mitogen-activated protein kinase. It has been shown that MAPK is transiently activated in Mos-independent manner soon after meiosis induction and phosphroylates CPEB on three amino acid residues, yet none of them is Ser174. However, experiments with an inhibitor of MEK, the kinase upstream of MAPK, have shown that early MAPK activation is necessary for CPEB Ser174 phosphorylation, implying that MAPK might either prime CPEB for subsequent activating phosphorylation on Ser174 by a different kinase, or MAPK activity might be required for activation of a kinase upstream of CPEB (Keady *et al*. 2007). Notably, an involvement of MAPK in CPEB-mediated translational activation was recently reported also in mouse oocytes (Sha *et al*. 2016).

Furthermore, calcium/calmodulin-dependent protein kinase II (CaMKII) has been shown to phosphorylate CPEB on Thr171 residue in mouse hippocampal neurons. In addition, CaMKII kinase activity in mouse neurons is necessary for translation of luciferase coding region fused to 3'UTR containing CPE (Atkins *et al.* 2004).

Altogether, more experiments need to be conducted to reveal the identity of kinase(s) involved in CPEB-mediated translational activation. This thesis aims to contribute to this effort by examining the possible role of MAPK in this process.

2.3.5 Cytoplasmic polyadenylation of cyclin B1 mRNA in maturing mouse and porcine oocytes

Cyclin B1, together with Cdk1, forms maturation-promoting factor (MPF), the major regulator of meiotic cell cycle. The kinase activity of MPF is required for meiosis progression and it is regulated by the level of cyclin B1 protein, as the amount of Cdk1 remains unchanged during meiosis (as described in more detail in section 2.2.1).

The synthesis of cyclin B1 protein is regulated by cytoplasmic polyadenylation of its mRNA in both mouse and porcine oocytes (Tay *et al*. 2000, Zhang *et al*. 2010a). Mouse cyclin B1 mRNA contains four CPE-like sequences in 3'UTR and undergoes moderate level of polyadenylation (~100 nucleotides) during the transition from the GV stage to metaphase I and robust polyadenylation between metaphase I and metaphase II (~250 nucleotides) (Tay *et al*. 2000). Two cyclin B1 transcript isoforms of different 3'UTR lengths were identified in porcine oocytes. The longer one possesses three hexanucleotide polyadenylation signals (PAS1-3) and five CPE-like sequences (Fig. S2). The short transcript is generated when PAS2 rather then PAS3 is recognized by nuclear CPSF which then governs the cleavage and polyadenylation of cyclin B1 pre-mRNA. The only CPE present in the 3'UTR of short isoform is fused to PAS2. Despite the difference in 3'UTR length and number and position of CPEs, the polyadenylation of both isoforms was detected only after 24 hours of maturation and continued until the end of maturation (Zhang *et al*. 2010a).

The described changes in cyclin B1 mRNA poly(A) tail length in maturing oocytes have been further confirmed by many other studies (Yang *et al*. 2010, Guzeloglu-Kayisli *et al*. 2012, Kotani *et al*. 2013, Komrskova *et al*. 2014, Liu *et al*. 2016, Sha *et al*. 2016). For this reason I decided to monitor the polyadenylation state of this mRNA as a marker of CPEB1-dependent cytoplasmic polyadenylation in this work.

3. AIMS OF THE THESIS

The aim of this thesis is to examine the role of mitogen-activated protein kinase (MAPK) in regulation of cytoplasmic polyadenylation of cyclin B1 mRNA in maturing mouse and porcine oocytes.

The specific objectives are:

- to examine the timing of MAPK activation and cyclin B1 mRNA cytoplasmic polyadenylation in maturing oocytes

- to evaluate the effect of MAPK inhibition on cytoplasmic polyadenylation of cyclin B1 mRNA in oocytes matured either with or without cumulus cells

- to achieve the above-mentioned objectives using both mouse and porcine oocytes.

4. MATERIAL AND METHODS

4.1 Mouse oocyte collection and culture

Laboratory mice (*Mus musculus*, outbred CD1 strain) were purchased from Velaz (Czech Republic). All mice were maintained and bred in the animal facility of IAPG AS CR under a 12:12-hr light:dark cycle. Ovaries were obtained from 4-6 weeks old mice intraperitoneally injected with 4 IU of pregnant mare's serum gonadotropin (PMSG; Folligon, MSD Animal Health) 42 hours prior to collection. PMSG is a hormone used to stimulate ovulation and increase a yield of oocyte isolation. Mice were euthanized by cervical dislocation and ovaries were excised and placed in a drop of preheated transfer medium (TM; see below for composition) supplemented with 100 μM of 3-isobutyl-1-methylxanthine (IBMX; Sigma, I5879) on a Petri dish. IBMX is a phosphodiesterase inhibitor and is used to prevent spontaneous resumption of meiosis. Ovaries were disrupted using two needles and oocytes were collected and transferred in a well of a 4-well cultivation dish containing 500 μl of EmbryoMax® Modified M16 Medium (M16; Merck Millipore, MR-016-D) supplemented with 100 μM of IBMX. The cultivation dish with M16 medium was pre-equilibrated in the incubator (Heracell 150, Thermo Scientific™) with a semi-opened lid for a minimum of 1 hour prior to use. The dish containing the oocytes was placed in the incubator for 15 min, cumulus cells were removed from the oocytes by gentle pipetting and the denuded oocytes were then further incubated for another 15 min. The denuded oocytes were transferred to a drop of preheated TM supplemented with 100 μM of IBMX on a Petri dish. Fully-grown oocytes with intact GV were selected and were either processed for *in vitro* maturation or, when a sample of GV stage oocytes was prepared, washed three times in 0.1% solution of polyvinyl alcohol (PVA; Sigma, P8136) in phosphate-buffered saline (PBS; see below for composition) (PVA/PBS), placed into a test tube and kept at -80°C. For maturation, oocytes were washed twice in TM (without IBMX) and transferred to a well of a cultivation dish containing 500 μl of pre-equilibrated M16 medium (without IBMX). The dish was placed in the incubator and the oocytes were let to mature at 37°C in a humidified atmosphere of 5% CO_2. Oocytes that had not undergone GVBD until 80 min of maturation were discarded. At the time of sample collection, which varied according to a design of an experiment (for details refer to the Results section), oocytes were transferred to a drop of TM containing 100 μM of IBMX on a Petri dish, washed three times in 0.1% (w/v) PVA/PBS, placed into a test tube and stored at -80°C. When samples for poly(A) tail assay were prepared, oocytes were frozen dry in a 1.5-ml PCR clean test tube. For western blotting, oocytes were frozen dry in an 0.5-ml sterile test tube. For *in vitro* kinase assay, oocytes were frozen in 5 μl of kinase lysis buffer (for composition see section 4.5) in an 0.5-ml sterile test tube.

For maturation of cumulus-enclosed oocytes (CEOs), CEOs were washed twice in TM without IBMX and immediately transferred to a well of a cultivation dish containing 500 µl of pre-equilibrated M16 medium without IBMX. The dish was placed in the incubator and the oocytes were let to mature. In contrast to cultivation of denuded oocytes, CEOs that had not undergone GVBD until 80 min of maturation were not discarded, since the presence of cumulus cells made it impossible to identify, whether GV is intact or not. Before sample collection, cumulus cells were removed by pipetting CEOs through a glass mini pipett with a diameter of about the diameter of the oocyte.

MOUSE TRANSFER MEDIUM		
100 mM	NaCl	
5.4 mM	KCl	
2 mM	$CaCl_2.2H_2O$	
0.5 mM	KH_2PO_4	
0.4 mM	$MgSO_4.7H_2O$	
11 mM	Glucose	
8.4 mM	HEPES	
13 mM	$NaHCO_3$	
1.8 mM	Sodium pyruvate	
0.1% (w/v)	Polyvinyl alcohol	
0.004% (w/v)	Penicilin	Biotika
0.006% (w/v)	Streptomycin	Sigma (S9137)
0.012% (w/v)	Amphotericin B	Sigma (A9528)
0.25% (w/v)	Bovine serum albumin (BSA)	Roche (10735078001)

PHOSPHATE-BUFFERED SALINE (PBS): 1 tablet (Sigma, P4417) was dissolved in 200 ml of deionized water. 10 mM phosphate buffer, 2.7 mM KCl, 137 mM NaCl, pH 7.4 at 25°C.

4.2 Porcine oocyte collection and culture

Porcine (*Sus scrofa*) ovaries were collected at a commercial slaughterhouse (Jatky Český Brod a.s., CZ) and transported in a vacuum flask to the laboratory. Oocytes were aspirated from follicles using a 5-ml syringe with a 21-gauge needle and collected in a glass tube. Once the oocytes sedimented to the bottom of the tube, follicular fluid was removed using a plastic Pasteur pipette and the oocytes were washed twice with preheated transfer medium (TM; see below for composition). The sedimented oocytes were resuspended in a small volume of transfer medium and poured on a Petri dish. Oocytes surrounded by compact cumuli were

selected and were processed either for collection of a sample of GV stage oocytes or for *in vitro* maturation. For collection of a sample of GV stage oocytes, oocytes in a small volume of TM were placed at the bottom of a narrow glass tube and vortexed for a few minutes to remove cumulus cells from oocytes. Cumulus-free oocytes were selected, washed three times in a 0.1% (w/v) PVA/PBS (for composition of PBS see section 4.1), placed into a test tube and kept at -80°C. For maturation, oocytes were washed twice in a drop of preheated M199 cultivation medium (M199; Gibco™, 21157029) and transferred to a well of a 4-well cultivation dish containing 500 µl of M199 cultivation medium supplemented with 10% (v/v) fetal bovine serum (FBS; Sigma, F0392), 2.6 IU of PMSG and 1.3 IU of human chorionic gonadotrophin (PG 600; MSD Animal Health). The cultivation dish with M199 medium was pre-equilibrated in the incubator (Galaxy® 48 S, New Brunswick™) with a semi-opened lid for a minimum of 1 hour prior to use. The dish was placed in the incubator and the oocytes were let to mature at 38.5°C in a humidified atmosphere of 5% CO_2. At the time of sample collection, which varied according to a design of an experiment (for details refer to the Results section), oocytes were transferred to a drop of a 0.1% (w/v) solution of hyaluronidase (Sigma, H3506) in TM. Hyaluronidase dissolves the intercellular matrix between the cumulus cells by hyaluronan degradation and in this way helps to remove the cumulus cells from the oocyte. After 30 s of hyaluronidase treatment, oocytes were washed twice in a drop of TM, placed in a small volume of TM at the bottom of a narrow glass tube and vortexed for one minute to remove the rest of cumulus cells attached to the oocytes. Cumulus-free oocytes were selected, washed three times in a 0.1% (w/v) PVA/PBS, placed into a test tube and stored at -80°C. When samples for poly(A) tail assay were prepared, oocytes were frozen dry in a 1.5-ml PCR clean test tube. For western blotting, oocytes were frozen dry in an 0.5-ml sterile test tube. For *in vitro* kinase assay, oocytes were frozen in 5 µl of kinase lysis buffer (for composition see section 4.5) in an 0.5-ml sterile test tube.

For maturation of denuded oocytes, cumulus cells were removed by pipetting CEOs through a glass mini pipett with a diameter of about the diameter of the oocyte. Cumulus-free oocytes were washed twice in a drop of preheated M199 cultivation medium and transferred to a well of a 4-well cultivation dish containing 500 µl of pre-equilibrated M199 cultivation medium supplemented wit 10% (v/v) FBS. The dish was placed in the incubator and the oocytes were let to mature under the same conditions as used for CEOs maturation. At the time of sample collection, oocytes were washed three times in a 0.1% (w/v) PVA/PBS and processed as was described for CEOs.

For evaluation of maturation stage, a group of at least 15 denuded oocytes was mounted between a glass slide and a coverslip. A small amount of a mixture of vaseline and beeswax was applied on the glass slide and by gently pressing down the coverslip, oocytes were

compressed between the coverslip and the glass slide (Fig. 5). The oocytes were fixed for at least 48 hours by placing the slide in a glass container containing fixative solution (for composition see below). Chromatin staining was performed with aceto-orcein staining solution (for composition see below) followed by washing with fixative solution. Oocytes were observed using bright-field microscopy (Leica DMI 6000 B, Leica Microsystems).

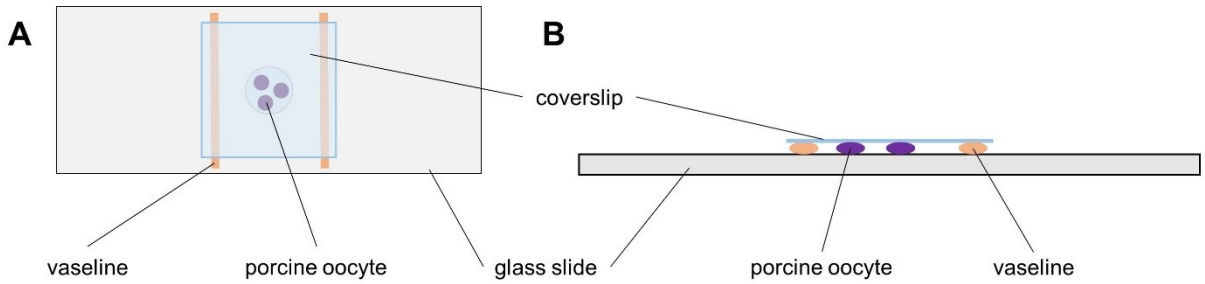

Fig. 5. Schematic drawing of porcine oocytes mounted on a slide.
An upper view (A) and a side view (B) of porcine oocytes mounted on a glass slide.

PORCINE TRANSFER MEDIUM: Same as mouse transfer medium but without BSA.

FIXATIVE SOLUTION: 75% (v/v) ethanol, 25% (v/v) acetic acid.

ACETO-ORCEIN STAINING SOLUTION: 2% (w/v) orcein (LOBA Feinchemie) and 1% (w/v) trisodium citrate in 50% (v/v) aqueous-acetic acid.

4.3 Inhibitor treatment

For inhibition of MAPK activity, GDC-0994 (Selleckchem, S7554) was used. GDC-0994 was dissolved in dimethyl sulfoxide (DMSO; Sigma, D8418), immediately aliquoted and stored at -80°C. Prior to oocyte cultivation, GDC-0994 was added to cultivation medium. The final concentration of DMSO in cultivation medium was 0.2% (v/v).

4.4 Poly(A) tail assay

Poly(A) tail (PAT) assay was done to determine the length of cyclin B1 mRNA poly(A) tail. It was performed as described by Salles and Strickland (1995) with minor modifications. The method is based on full-length reverse transcription of polyadenylated mRNAs during which an anchor sequence is added at the very end of the poly(dT) tract in cDNA. This cDNA is then used as a template for PCR amplification together with a primer specific for the mRNA of interest and the oligo(dT)-anchor as the reverse primer. The poly(A) tail length can be

concluded from the size of the PCR product. Essentially, the longer the poly(A) tail was, the bigger PCR product it yields. An overview of the method is shown in Fig. 6. Several aspects of PAT assay, such as RNA elution volume, amount of RNA used for reverse transcription, amount of cDNA used as template for PCR amplification and duration of DNA polyacrylmide gel electrophoresis, were extensively optimized to minimize the number of oocytes per sample.

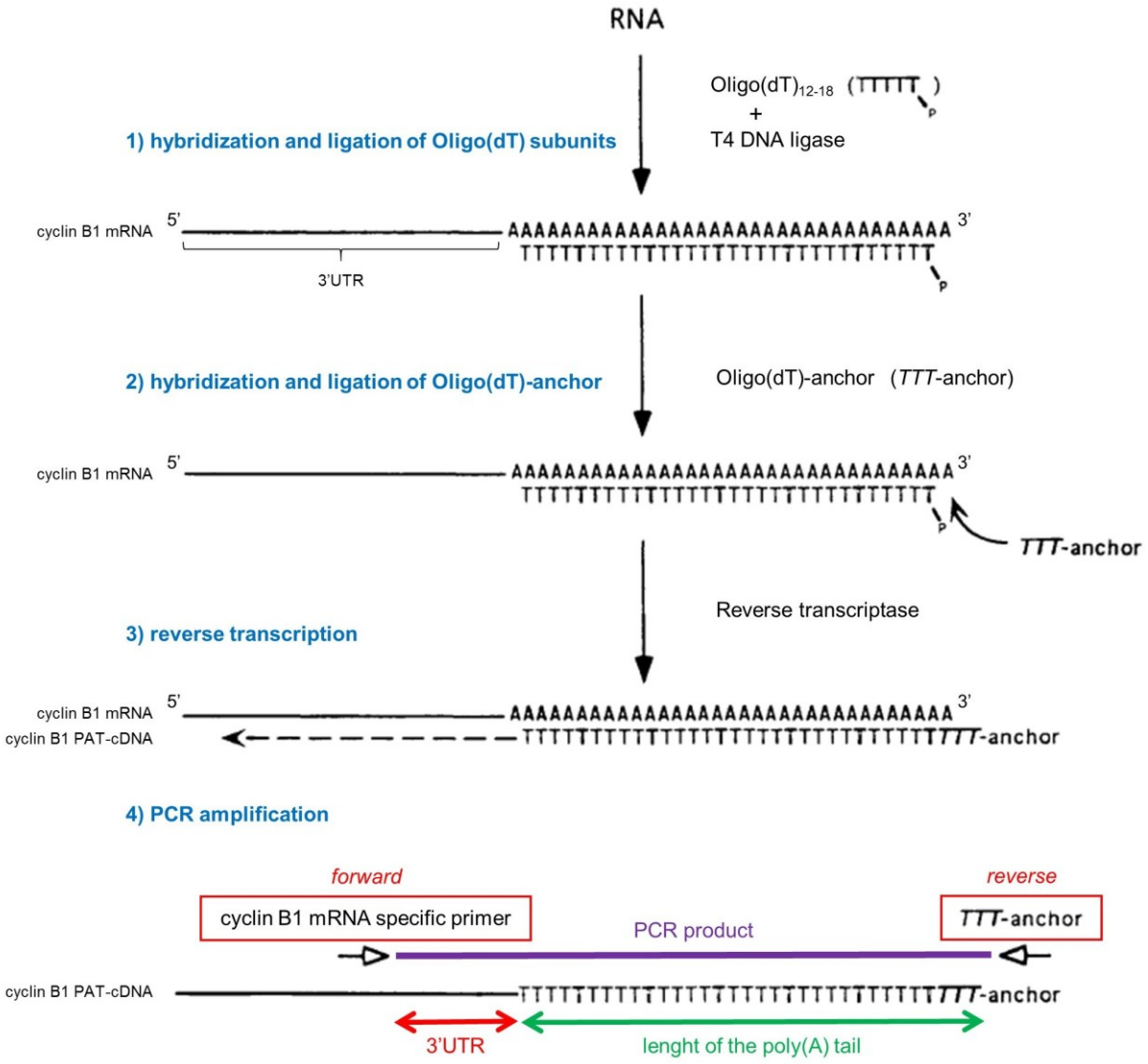

Fig. 6. Overview of the poly(A) tail assay. Adapted from Salles and Strickland (1995).

Total RNA is isolated from a sample and the poly(A) tails of mRNAs are saturated by hybridization of deoxythimidine monophosphate oligonucleotides (oligo(dT)) of different lengths ranging from 12 to 18 dT. Oligo(dT)$_{12\text{-}18}$ bind randomly throughout the poly(A) tail and when two oligo(dT) hybridize next to each other, they are ligated together by T4 DNA ligase. Oligo(dT)-anchor is eventually added, it hybridizes to the very end of poly(A) tail and is ligated to the rest of poly(dT) strand. The mRNA is reverse transcribed using poly(T)-anchor strand as a primer. PCR amplification is performed using a forward primer specific for cyclin B1 mRNA and oligo(dT)-anchor is used as the reverse primer. The size of the PCR product is determined by comparison with a DNA ladder after electrophoresis. The length of the poly(A) tail (green line) is estimated by reducing the size of the PCR product (purple line) by size of the part of the PCR product amplified from 3'UTR (red line).

4.4.1 RNA isolation

Total RNA was isolated from groups of 10 oocytes using RNeasy Plus Micro Kit (QIAGEN, 74034) accoring to the following protocol.

1) Oocytes were lysed by the addition of 350 µl of Buffer RLT Plus supplemented with 1% (v/v) 2-Mercaptoethanol (Sigma, M3148) and vortexing for 15 s. The lysate was spun down shortly.

2) The lysate was transferred to a gDNA Eliminator spin column placed in a 2-ml collection tube and centrifuged for 30 s at 12,000 x g. The column was discarded.

3) 350 µl of 70% (v/v) ethanol was added to the flow-through, the whole volume was transferred to an RNeasy MinElute spin column placed in a 2 ml collection tube and centrifuged for 30 s at 12,000 x g. The flow-through was discarded.

4) 700 µl of Buffer RW1 was added to the RNeasy MinElute spin column and centrifuged for 30 s at 12,000 x g. The flow-through was discarded.

5) 500 µl of Buffer RPE was added to the RNeasy MinElute spin column and centrifuged for 30 s at 12,000 x g. The flow-through was discarded.

6) 500 µl of 80% (v/v) ethanol was added to the RNeasy MinElute spin column and centrifuged for 2 min at 12,000 x g. The collection tube with the flow-through was discarded.

7) The RNeasy MinElute spin column was placed in a new collection tube and centrifuged for 5 min at full speed with an open lid. The collection tube was discarded.

8) The RNeasy MinElute spin column was placed in a new 1.5-ml tube, 17 µl of RNase-free water was added and after 1 min incubation it was centrifuged for 1 min at full speed. Due to the dead volume of the spin column, 15 µl of RNA-containing water was yielded.

RNA isolation was performed at a room temperature. Once the RNA was eluted it was immediately placed on ice and 7 µl of RNA was transferred to a PCR tube with a dome cap. The rest of RNA was stored at -80°C.

4.4.2 Reverse transcription

1) 1 µl of Oligo(dT)$_{12-18}$ Primer (Invitrogen™, 18418012; 25 ng/µl) was added to 7 µl of RNA in a PCR tube. The tube was placed in the Veriti® 96-Well Thermal Cycler (Applied Biosystems™) and the following program was started.

REVERSE TRANSCRIPTION PROGRAM			
Step	**Temperature**	**Time**	**Purpose**
1	65°C	5 min	RNA denaturation
2	42°C	30 min	Oligo(dT)$_{12-18}$ hybridization and ligation
3	12°C	2 hr	Oligo(dT)-anchor hybridization and ligation
4	42°C	1 hr	Reverse transcription
5	70°C	30 min	Reverse transcriptase and ligase inactivation

2) Once the temperature reached 42°C (step 2), 12 µl of reverse transcription mastermix (for composition see the table below) preheated to 42°C was added and mixed well by pipetting. The tube was not taken out of the thermal cycler when the mastermix was being added.

REVERSE TRANSCRIPTION MASTERMIX		
4 µl	5x First-strand buffer: 250 mM Tris-HCl pH 8.3, 375 mM KCl, 15 mM $MgCl_2$	Invitrogen™ (18080093)
1 µl	0.1 M dithiothreitol	Invitrogen™ (18080093)
1 µl	RNaseOUT™ Ribonuclease Inhibitor (40 U/µl)	Invitrogen™ (10777019)
1 µl	dNTP; 10 mM each deoxynucleotide	NEB (N0447)
1 µl	10 mM ATP	NEB (P0756)
1 µl	T4 DNA Ligase (400 U/µl)	NEB (M0202S)
3 µl	RNase-free water	

3) At the end of step 2, prior to a decrease of the temperature to 12°C, 2 µl of 10 µM Oligo(dT)-anchor (for sequence see the list of primers in section 4.4.3) was added and mixed well by pipetting. The tube was not taken out of the thermal cycler when Oligo(dT)-anchor was being added.

4) Once the temperature reached 42°C again (step 4), 1 µl of SuperScript™ III Reverse Transcriptase (Invitrogen™, 18080093; 200 U/µl) was added and mixed well by pipetting. The tube was not taken out of the thermal cycler when reverse transcriptase was being added.

5) When the PCR program finished the tube with PAT-cDNA was taken out of the thermal cycler and was stored at 4°C until the next day.

4.4.3 Polymerase chain reaction (PCR)

For PCR amplification, PAT-cDNA was used as a template, Oligo(dT)-anchor was used as a reverse primer and an oligonucleotide complementary to cyclin B1 mRNA was used as a forward primer. The forward primer used to detect polyadenylation of mouse cyclin B1 mRNA

was designed to anneal to cyclin B1 3'UTR and yielded one PCR product representing the transcript generated by cleavage of cyclin B1 pre-mRNA just downstream of PAS4 (Fig. S1). The forward primer used to detect polyadenylation of porcine cyclin B1 mRNA was designed to anneal to cyclin B1 coding region and yielded two PCR products representing the long and short transcript isoforms generated by cleavage of cyclin B1 pre-mRNA just downstream of PAS3 and PAS2, respectively (Fig. S2). In this thesis I only show the results of poly(A) tail assay of the short isoform of porcine cyclin B1 transcript.

PRIMERS USED IN THIS STUDY		
cyclin B1 mouse	CAAGTGCATTCTCTCAGTGCCCTCCACAGTGT	NM_172301.3
cyclin B1 pig	GCATTTTCTTCGGAGAGCATCCAAGATT	NM_001170768.1
Oligo(dT)-anchor	GCGAGCTCCGCGGCCGCGTTTTTTTTTTT	Salles and Strickland (1995)

The PCR reaction mixture was prepared in a PCR tube with a dome cap as follows. As a negative control, reaction mixture without PAT- cDNA template was used. Samples were amplified in a thermal cycler according to the PCR program below. When the program finished, samples were taken out of the thermal cycler, spun down and stored at 4°C until the gel for electrophoresis was prepared.

PCR REACTION MIXTURE		
2 µl	10X ThermoPol Reaction Buffer 200 mM Tris-HCl, 100 mM $(NH_4)_2SO_4$, 100 mM KCl, 20 mM $MgSO_4$, 1% Triton® X-100, pH 8.8	NEB (M0267S)
0.6 µl	dNTP; 10 mM each deoxynucleotide	NEB (N0447)
1 µl	10 µM forward primer	Generi Biotech
1 µl	10 µM Oligo(dT)-anchor	Generi Biotech
0.1 µl	*Taq* DNA Polymerase (5 U/µl)	NEB (M0267S)
13.3 µl	RNase-free water	
2 µl	PAT-cDNA	

PCR PROGRAM			
Step	**Temperature**	**Time**	**No. of Cycle**
Initial denature	94°C	2 min	1
Denature	94°C	45 s	34
Annealing	60°C	45 s	
Extension	72°C	60 s	
Final Extension	72°C	5 min	1

4.4.4 DNA polyacrylmide gel electrophoresis

Amplified PCR products were resolved on 5% polyacrylamide gel. For gel characteristics and composition of gel solution see the tables below.

Type of gel	homecast
Buffer system	Tris-Borate-EDTA (TBE) continuous
Gel size	13.5 cm x 10.5 cm x 1.5 mm
T value*	5%
C value**	3.3%

* total % concentration (w/v) of acrylamide and bisacrylamide in the gel
** % concentration (w/w) of bisacrylamide in the mixture of acrylamide and bisacrylamide

DNA-PAGE GEL SOLUTION		
16.7% (v/v)	Acrylamide/bis-acrylamide, 30% solution	Sigma (A3574)
20% (v/v)	5x Tris-borate-EDTA (TBE) buffer	
0.1% (w/v)	Ammonium persulfate (APS)	Sigma (A3678)
0.1% (v/v)	*N,N,N′,N′*-Tetramethylethylenediamine (TEMED)	Sigma (T9281)

The gel was prepared using an apparatus consisting of two glass plates separated on sides by plastic spacers, inserted into a tight plastic bag and mounted into a holder. The gel solution was poured into the gap between the glass plates until an overflow and a plastic well-forming comb was inserted. After 30 min the comb was removed and the wells were washed with deionized water. The gel was mounted in Owl™ Dual-Gel Vertical Electrophoresis aparatus (Thermo Scientific™, P9DS). When just one gel was run, a plastic substitute was inserted to the electrophoresis apparatus to form the upper buffer chamber. Both buffer chambers were filled with Tris-borate-EDTA (TBE) buffer (for composition see below).

Just before sample loading, 4 µl of DNA Gel Loading Dye (6X) (Thermo Scientific™, R0611) was added to each sample and mixed well by pipetting. The samples were loaded in the wells of the gel. To assess the molecular sizes of DNA fragments, 2 µl of GeneRuler 1 kb Plus DNA Ladder, ready-to-use (Thermo Scientific™, SM1333) was loaded next to the samples. The gel was run at 120 V at temperature of 10°C for appx. 3 hours. Following electrophoresis, the gel was stained with 0.005% (v/v) GelRed™ (Biotium, 41001 - 41003-T) in TBE for 30 min. The PCR products were visualized and imaged using Kodak Gel Logic 100/200 Camera (Eastman Kodak Company) and KODAK MI SE software.

5x TRIS-BORATE-EDTA (TBE)		
0.45 M	Tris base	Roche (10708976001)
0.45 M	Boric acid	Sigma (B6768)
2% (v/v)	0.5 M EDTA pH 8.0	Sigma (E5134)

4.5 Double *in vitro* kinase assay

The kinase activities of both Cdk1 and MAPK were determined in a single assay via their capacity to phosphorylate external substrates histone H1 and myelin basic protein (MBP), respectively, according to Motlik *et al*. (1996). This assay is based on *in vitro* phosphorylation of an external substrate by kinase(s) present in a lysate of oocytes using ATP labeled on the gamma phosphate group with ^{32}P.

Oocytes collected for *in vitro* kinase assay were stored in 5 µl of kinase lysis buffer (for composition see below) at -80°C. Oocytes were lysed by three rounds of thawing (at room temperature) and freezing (by placing the tube to a cooled freezing rack). After the addition of 5 µl of double kinase buffer (for composition see below) the kinase reaction was conducted at 30°C for 30 min. The reaction was terminated by the addition of 12.5 µl of double-strength concentrated reducing sample buffer (Laemmli 1970; for composition see section 4.6.1). The phosphorylated substrates were resolved by sodium dodecyl sulfate (SDS) polyacrylamide gel electrophoresis (PAGE) (for details see section 4.6). After electrophoresis the resolving part of the gel was stained with Coomassie Brilliant Blue R250 solution (for composition see below) at room temperature for 30 min with gentle shaking. To clear the gel matrix of the Coomassie dye, the gel was incubated in the destain solution (for composition see below) at room temperature with gentle shaking. The destain solution was changed twice and the third wash was done overnight. To avoid cracking of the gel during drying, the gel was incubated in 50% (v/v) glycerol in destain solution at room temperature for 1 hour with gentle shaking. The gel was dried using a dry-heat vacuum pump. During the drying procedure the gel was placed on a sheet of filter paper and as the gel was dehydrated it sticked to the paper which then provided a mechanical support. The gel was exposed to a storage phosphor screen inside a exposure cassette for 20 hours. Phosphorylated substrates were visualized by FujiFilm BAS-25 Photo Scanner (FujiFilm Life Science) and the kinase activiy was quantified using Aida Image Analyzer software (Raytes).

KINASE LYSIS BUFFER		
0.001% (w/v)	Leupeptin	Roche, 1017128
0.001% (w/v)	Aprotinin	Roche, 10236624001
10 mM	p-nitrophenyl phosphate	Aldrich, N2200-2
20 mM	β-glycerophosphate	Sigma, G9422
0.1 mM	Sodium orthovanadate	Sigma, S6508
5 mM	EGTA	Sigma-Aldrich, E4378
1 mM	Benzamidine	Aldrich, 12072
1 mM	AEBSF	Sigma-Aldrich, A8456

DOUBLE KINASE BUFFER		
50% (v/v)	4x H1 kinase buffer	
2.2 µM	Protein kinase inhibitor	Sigma, P0300
0.6 mM	ATP	Sigma, A7699
0.05% (w/v)	Histone H1	Roche, 10223549001
0.1% (w/v)	Myelin basic protein	Sigma, M1891
1 mCi/ml	[γ-^{32}P]ATP	Hartmann Analytic, FP-501

4x H1 KINASE BUFFER		
0.012% (w/v)	Leupeptin	
0.012% (w/v)	Aprotinin	
48 mM	p-nitrophenyl phosphate	
180 mM	β-glycerophosphate	
9.2 mM	Sodium orthovanadate	
48 mM	EGTA	
4 mM	Benzamidine	
4 mM	AEBSF	
48 mM	$MgCl_2$	
0.4 mM	EDTA	Sigma, E6511
8 mM	Sodium fluoride	
3.2 mM	Dithiothreitol	Sigma, 43817
0.4% (w/v)	Polyvinyl alcohol	Sigma-Aldrich, P8136
80 mM	MOPS, pH 7.2	Sigma, M3183

COOMASSIE BRILLIANT BLUE R250 SOLUTION: 0.1% (w/v) Coomassie Brilliant Blue R250 (Sigma, 27816), 40% (v/v) methanol, 10% (v/v) acetic acid.

DESTAIN SOLUTION: 40% methanol (v/v), 10% (v/v) acetic acid.

4.6 SDS polyacrylamide gel electrophoresis (SDS-PAGE)

Three different types of SDS polyacrylamide gels and electrophoretic conditions were used depending on the purpose of protein electrophoresis. When phosphorylated and unphosphorylated forms of MAPK were resolved, a homecast polyacrylamide gel containing a modified ratio of acrylamide and bisacrylamide (C value of 1%) was used (4.6.1). When proteins other then MAPK were resolved, a precast Invitrogen NuPAGE™ gel was used (4.6.3). When *in vitro* kinase assay substrates were resolved, a homecast polyacrylamide gel containing a standard ratio of acrylamide and bisacrylamide (C value of 2.6%) was used (4.6.2).

Both types of homecast gels were prepared using the same apparatus consisting of two glass plates separated on sides by plastic spacers, inserted into a tight plastic bag and mounted into a holder. Resolving gel solution (for composition see 4.6.1 and 4.6.2) was poured into the gap between the glass plates until it reached appx. 3/4 of the plate height. The gel solution was overlaid with 1.5 ml of butanol to ensure a horizontal interface between the resolving and stacking gels and the gel solution was let to polymerize. After 30 min butanol was poured out and the gap between the glass plates was washed twice with deionized water. Excess water was blotted off with a filter paper. Stacking gel solution (for composition see 4.6.1) was poured on the top of the resolving gel until an overflow and a plastic well-forming comb was inserted. After 30 min the comb was removed and the wells were washed with deionized water. At this point the gel was either stored at 4°C with the wells filled with deionized water or it was taken off the plastic bag, washed with deionized water and used for electrophoresis. The gel was mounted in Owl™ Dual-Gel Vertical Electrophoresis aparatus (Thermo Scientific™, P9DS). When just one gel was run, a plastic substitute was inserted to the electrophoresis apparatus to form the upper buffer chamber. Both buffer chambers were filled with running buffer (for composition see below). For electrophoresis specifications refer to following sections.

RUNNING BUFFER		
25 mM	Tris base	Roche (10708976001)
200 mM	Glycine	Carl Roth (3908.2)
3 mM	Sodium dodecyl sulfate (SDS)	Sigma-Aldrich (L6026)

4.6.1 Homecast gel for resolution of differently phosphorylated forms of MAPK

Type of gel	homecast
Buffer system	Tris-glycine discontinuous
Resolving gel size	13.5 cm x 9 cm x 1.5 mm
Resolving gel T value*	10.5%
Resolving gel C value**	1%

* total % concentration (w/v) of acrylamide and bisacrylamide in the gel
** % concentration (w/w) of bisacrylamide in the mixture of acrylamide and bisacrylamide

Oocyte samples were lysed in 15 µl of reducing sample buffer (Laemmli 1970; for composition see below) and heated at 100°C for 3 min. The samples were loaded in the wells of the gel. To assess the molecular sizes of proteins, 1.5 µl of Precision Plus Protein™ Dual Color Standards (BIO-RAD, 1610374) was loaded next to the samples. The gel was run at 175 V at temperature of 10°C for appx. 5 hours. The electrophoresis was stopped when the 25 kDa band of the protein marker almost reached the bottom line of glass plates.

REDUCING SAMPLE BUFFER		
0.8 M	Sodium dodecyl sulfate (SDS)	Sigma-Aldrich (L6026)
25% (v/v)	Glycerol	Sigma (G5516)
5% (v/v)	2-Mercaptoethanol	Aldrich (M6250)
62.5% (v/v)	1 M Tris-HCl pH 6.8	
0.01% (w/v)	Bromphenol Blue	Sigma-Aldrich (B0126)

STACKING GEL		
17% (v/v)	Acrylamide/bis-acrylamide, 30% solution	Sigma (A3699)
25% (v/v)	0.5 M Tris-HCl pH 6.8	
0.1% (w/v)	Sodium dodecyl sulfate (SDS)	Sigma-Aldrich (L6026)
0.1% (w/v)	Ammonium persulfate (APS)	Sigma (A3678)
0.1% (v/v)	*N,N,N′,N′*-Tetramethylethylenediamine (TEMED)	Sigma (T9281)

RESOLVING GEL		
0.1% (w/v)	Methylene bisacrylamide	Serva (29195)
10.4% (w/v)	Acrylamide	Serva (10674)
25% (v/v)	1.5 M Tris-HCl pH 8.8	
0.1% (w/v)	Sodium dodecyl sulfate (SDS)	Sigma-Aldrich (L6026)
0.06% (w/v)	Ammonium persulfate (APS)	Sigma (A3678)
0.06% (v/v)	*N,N,N′,N′*-Tetramethylethylenediamine (TEMED)	Sigma (T9281)

4.6.2 Homecast gel for *in vitro* kinase assay

Type of gel	homecast
Buffer system	Tris-glycine discontinuous
Resolving gel size	13.5 cm x 9 cm x 1 mm
Resolving gel T value*	15%
Resolving gel C value**	2.6%

* total % concentration (w/v) of acrylamide and bisacrylamide in the gel
** % concentration (w/w) of bisacrylamide in the mixture of acrylamide and bisacrylamide

The *in vitro* kinase reaction was terminated by the addition of 12.5 µl of double-strength concentrated reducing sample buffer (for composition see section 4.6.1) and heating at 100°C for 4 min. The samples were loaded in the wells of the gel. To assess the molecular sizes of proteins, 10 µl of Prestained Protein Marker (NEB, P7708S) was loaded next to the samples. The gel was run at 50 mA at room temperature for appx. 1.5 hour. The electrophoresis was stopped when the sharp yellow line of radiolabeled ATP almost reached the end of the gel.

STACKING GEL: For composition see section 4.6.1.

RESOLVING GEL		
50% (v/v)	Acrylamide/bis-acrylamide, 30% solution	Sigma (A3699)
25% (v/v)	1.5 M Tris-HCl pH 8.8	
0.1% (w/v)	Sodium dodecyl sulfate (SDS)	Sigma-Aldrich (L6026)
0.1% (w/v)	Ammonium persulfate (APS)	Sigma (A3678)
0.04% (v/v)	*N,N,N′,N′*-Tetramethylethylenediamine (TEMED)	Sigma (T9281)

4.6.3 Precast Invitrogen NuPAGE™ gel

Type of gel	precast
Buffer system	Bis-Tris discontinuous
Resolving gel size	8 cm x 6 cm x 1 mm
Resolving gel T value*	4-12%

* total % concentration (w/v) of acrylamide and bisacrylamide in the gel
** % concentration (w/w) of bisacrylamide in the mixture of acrylamide and bisacrylamide

Oocyte samples were lysed in 10 µl of reducing NuPAGE sample buffer (for composition see below) and heated at 100°C for 3 min. The samples were loaded in the wells of the NuPAGE™ 4-12% Bis-Tris Protein Gel (Invitrogen™, NP0321) mounted in the XCell SureLock® Mini-Cell (Invitrogen™, EI0001) electrophoresis chamber system. Both buffer chambers were filled with NuPAGE® MES SDS Running Buffer (Invitrogen™, NP0002) and 500 µl of NuPAGE® Antioxidant (Invitrogen™, NP0005) was added to the buffer within the upper buffer chamber

prior to sample loading. To assess the molecular sizes of proteins, 1.5 µl of Precision Plus Protein™ Dual Color Standards was loaded next to the samples. The gel was run at 175 V at room temperature for appx. 1.5 hour. The electrophoresis was stopped when the downmost band of the protein marker run out of the gel.

NuPAGE SAMPLE BUFFER: 25% (v/v) NuPAGE® LDS Sample Buffer (4X) (Invitrogen™, NP0007), 10% (v/v) NuPAGE® Sample Reducing Agent (10X) (Invitrogen™, NP0004).

4.7 Western blotting

After electrophoresis the stacking part of the gel was removed and the resolving gel was incubated in towbin buffer (pH 9.2; for composition see below) for 10 min with gentle shaking. A piece of Immobilion-P Membrane (Merck Millipore, IPVH00010) of the size of the resolving gel was doused with methanol and rinsed with towbin buffer. Two pieces of extra thick blot filter paper were soaked in towbin buffer and the “blotting sandwich” was prepared. Proteins were transferred from the gel to the membrane using a semidry blotting system (Fastblot B43, Biometra) either for 30 min at 275 mA (small precast gel) or for 45 min at 499 mA (large homecast gels). The blotting machine was cooled down during the transfer. The membrane was blocked, depending on the used antibody, in 10% (v/v) gelatin (Sigma, G7765) or 1% (w/v) skimmed milk dissolved in 0,05% (v/v) TWEEN® 20 (Sigma-Aldrich, P1379)-Tris-buffered saline (TTBS; for composition of TBS see below) for at least 1 hour at room temperature. Following the incubation in blocking solution, the membrane was placed in a 50-ml falcon tube containing 2 ml of diluted primary antibody. The membrane was incubated with the primary antibody at 4°C overnight on a tube roller. After three 10-min washes in TTBS, the membrane was incubated with a horseradish peroxidase-conjugated donkey anti-mouse (Jackson ImmunoResearch, 715-035-151) or anti-rabbit (Jackson ImmunoResearch, 711-035-152) secondary antibody in 1:7,500 dilution in 1% milk/TTBS for 1 hour at room temperature. For the list of used antibodies see Table 1.

Target protein	Producer and catalog number	Source	Blocking buffer	Dilution	II. Ab dilution buffer
MAPK3/1	Santa Cruz (sc-94)	R	10% gelatine	1:1000 in TTBS	TTBS
Phospho-p90/RSK (Thr359/Ser363)	Cell Signaling (#9344)	R	1% milk	1:500 in 1% milk	1% milk
Phospho-eIF2α (Ser51)	Cell Signaling (#9721)	R	1% milk	1:500 in 1% milk	1% milk
GAPDH	Sigma (G9545)	R	1% milk	1:10,000 in 1% milk	1% milk
Cyclin B1	Thermo Scientific (MS-338)	M	1% milk	1:500 in 1% milk	1% milk

Table 1. Primary antibodies used in this study. II. Ab, secondary antibody; M, mouse; R, rabbit

After three 10-min washes in TTBS immunodetected proteins were visualized by chemiluminescence using ECL™ Prime Western Blotting System (GE Healthcare, RPN2232). The membrane was placed protein side up on a glass plate and was covered with a mix of detection solution A (luminol) and B (peroxide) in a ratio of 1:1. After 5 min the membrate was placed into an X-ray film cassette and a sheet of X-ray film (Thermo Scientific™, 34091) was placed on top of the membrane. The membrane was exposed to the film inside the closed cassette for various periods of time depending on the primary antibody used and ranging from 30 s to 1 hour. The X-ray film was then developed, dried and scanned using a GS-800™ calibrated densitometer (BIO-RAD).

TOWBIN BUFFER pH 9.2		
50 mM	Tris base	Roche (10708976001)
40 mM	Glycine	Carl Roth (3908.2)
10% (v/v)	Methanol	Lachner (20038-AT0)

TRIS-BUFFERED SALINE (TBS): 0.8% (w/v) NaCl, 1% (v/v) 2 M Tris-HCl pH 7.6.

4.8 Immunocytochemistry

Mouse oocytes were washed three times in a drop of 0.1% (w/v) PVA/PBS (for composition of PBS see section 4.1) and fixed in a drop of 4% (w/v) paraformaldehyde (Alfa Aesar, 433689M) in PBS for 20 min on a Petri dish. Fixed oocytes were washed three times in a drop of 0.1% (w/v) PVA/PBS and transferred to a well of 24-well plate containing 800 µl of 0.1% Triton-X-100

(Sigma, T8787) in PBS. Oocytes were permeabilized in Triton for 10 min with slow shaking and subsequently transferred to a new well of 24-well plate containing 1 ml of 0.1% (w/v) PVA/PBS and incubated for 5 min with slow shaking. Oocytes were transferred to a well of 96-well plate containing 100 µl of diluted primary antibody directed against acetylated α-tubulin (Sigma, T6793; 1:150 dilution in PVA/PBS; raised in mouse) and incubated overnight at 4°C with slow shaking. The next day, oocytes were washed twice for 15 min in 0.1% (w/v) PVA/PBS and transferred to a well of 24-well plate containing 500 µl of diluted donkey anti-mouse secondary antibody conjugated to Alexa Fluor® 488 (Invitrogen™; 1:250 dilution in PVA/PBS) and incubated for 1 hour at room temperature with slow shaking. The plate was covered with aluminium foil to prevent photobleaching. Oocytes were then washed twice for 15 min in 0.1% (w/v) PVA/PBS and transferred to an 18-µl drop of Vectashield Antifade Mounting Medium with DAPI (Vector Labs, H-1200). A coverslip was placed on the drop and the mounted slide was kept at 4°C for one hour followed by sealing the coverslip around the perimeter with nail polish. Oocytes were visualized using a Leica SP5 inverted confocal microscope (Leica Microsystems) in 8 bit depth. Images were assembled in LEICA LasAFX software (Leica Microsystems).

4.9 Statistical analysis

Mean and s.d. values of mouse oocyte maturation rate were calculated using MS Excel, statistical significance of the differences between the groups was tested using Student's t-test (program R; www.r-project.org) and $p < 0.05$ was considered as statistically significant.

5. RESULTS

5.1 Cytoplasmic polyadenylation of cyclin B1 mRNA precedes MAPK activation in maturing mouse oocytes

Both MAPK activation and cyclin B1 mRNA polyadenylation during mouse oocyte maturation have already been described (Verlhac *et al*. 1993, Tay *et al*. 2000). However, whether these two events occur simultaneously or one precedes the other, and whether MAPK might be involved in cyclin B1 mRNA polyadenylation, has not yet been elucidated. This question was addressed by investigating MAPK activation and cyclin B1 mRNA polyadenylation in parallel and the results are presented in this section.

Mouse oocytes were allowed to reinitiate meiosis and samples were collected at the following time points of maturation: at the beginning of maturation (fully-grown GV stage oocytes), at 80 minutes of maturation (right after GVBD) and at 3 and 6.5 hours (corresponding to pro-MI and MI stages, respectively) as well as 12 hours (corresponding to MII stage) of maturation. Two samples at each time point were collected. One of them was processed for western blotting to examine the phosphorylation state and the activity of MAPK, the other one was processed for the poly(A) tail (PAT) assay to assess the level of cyclin B1 mRNA polyadenylation. The results presented here are representative of three independent cultivations and sample collections.

As shown by western blot analysis, there were two bands representing MAPK3 (44 kDa) and MAPK1 (42 kDa) present in the samples of GV and GVBD oocytes (Fig. 7A, lane 1 and 2). At 3 hours of maturation an upward mobility shift of both bands occured as a result of MAPK phosphorylation (Fig. 7A, lane 3). By 6.5 hours of maturation almost all MAPK proteins had shifted to their slowly migrating forms and remained phosphorylated throughout the rest of the maturation period (Fig. 7A, lanes 4 and 5).

In order to verify whether MAPK phosphorylation was linked to its activation, the presence of the phosphorylated form of MAPK substrate, p90/RSK, was examined. To that aim the western blot membrane was cut and the lower part was probed with an antibody against MAPK while the upper part was probed with an antibody detecting p90/RSK protein phosphorylated at Thr348/Ser352 (sites phosphorylated by MAPK). The phosphorylated form of p90/RSK (P-p90/RSK) was not detected until 3 hours after the start of maturation, which corresponded to the first detection of MAPK phosphorylation (Fig. 7A, lane 3). The P-p90/RSK band present in the sample of MII oocytes was rather faint, most likely because of some technical problem during protein transfer from the gel onto the membrane in this particular area (Fig. 7A, lane 5).

In parallel, changes in the level of cyclin B1 mRNA polyadenylation were analyzed. The poly(A) tail of cyclin B1 mRNA was elongated as soon as the GVBD occured (Fig. 7B, lane 2) and the elongation increased gradually until the MII stage (Fig. 7B, lane 3 - 5).

These results show that cytoplasmic polyadenylation of cyclin B1 mRNA precedes MAPK activation in maturing mouse oocytes, implying that MAPK activity is not required for the activation of cytoplasmic polyadenylation.

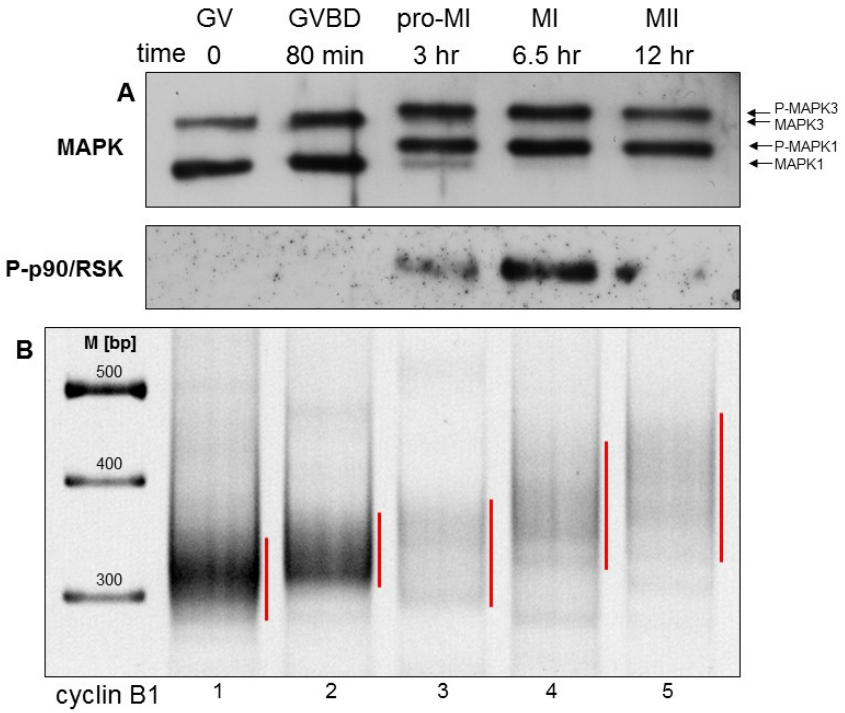

Fig. 7. Cytoplasmic polyadenylation of cyclin B1 mRNA occurs at GVBD, whereas MAPK activation is not detected until at 3 hours of oocyte maturation.

Oocytes were cultivated for 12 hours and samples of different stages of meiotic maturation were collected. Lane 1, fully-grown GV stage oocytes; lane 2, oocytes taken at GVBD after 80 min of cultivation; lane 3, 4 and 5, oocytes collected at 3, 6.5 and 12 hours of cultivation, respectively.
A: Western blot results showing the level of both phosphorylated and unphosphorylated forms of MAPK and the level of P-p90/RSK (representing MAPK activity). n = 15 oocytes per sample.
B: PAT assay results showing the level of cyclin B1 mRNA polyadenylation. The polyadenylation is highlighted by red lines next to each lane. n = 15 oocytes per sample. M, 1 kb DNA Ladder.
GV, germinal vesicle; GVBD, germinal vesicle breakdown; MI/II, metaphase I/II; P, phospho; pro-MI, prometaphase I.

5.2 GDC-0994 proves to be potent inhibitor of MAPK activity

To investigate whether MAPK activity is required for cytoplasmic polyadenylation of cyclin B1 mRNA in mouse oocytes, MAPK was inhibited by GDC-0994 compound. GDC-0994, in contrast to the most widely used compound U0126 which reduces MAPK activity indirectly by targeting its upstream kinase MEK, targets specifically MAPK and inhibits both its activating phosphorylation and activity (according to the information provided by the manufacturer, Selleckchem company).

Several concentrations of GDC-0994 were tested for their capacity to inhibit both MAPK activating phosphorylation and its activity. The ability of GDC-0994 to affect Cdk1 activity and/or to induce cellular stress response, measured by the level of eukaryotic translation initiation factor 2α (eIF2α) phosphorlyation, was monitored as well. The inhibition of Cdk1 activity and the induction of stress response are undesired potential side-effects as they lead to meiosis resumption block and global protein synthesis inhibition, respectively. For more information about eIF2α phosphorylation and its effect on translation see Wek *et al.* (2006).

Mouse oocytes were cultivated in the medium containing 50, 100 or 200 μM GDC-0994 for 7.5 hours. Some oocytes were cultivated in the inhibitor-free medium as a control. All three tested concentrations proved to be highly effective in reducing MAPK activity as shown by no P-p90/RSK present in the extracts from GDC-0994-treated oocytes (Fig. 8A). This result was also confirmed by the *in vitro* kinase assay (Fig. 8B). In this assay, samples were evaluated for their ability to phosphorylate the MAPK substrate, MBP, as well as the Cdk1 substrate, histone H1. Notably, low level of phosphorylation of both substrates could be seen in the sample of GV stage oocytes even though both MAPK and Cdk1 are inactive at this stage. This phosphorylation could be most likely attributed to other protein kinases as both substrates are full-size proteins containing also other than MAPK and Cdk1 phosphorylation sites (Pearson and Kemp 1991). For this reason, the obtained values of kinase activity were first reduced by the value measured in the GV sample. Then the value measured in the control sample was set as 100% and the values measured in the GDC-0994-treated samples were normalized to control activity. This was done for both Cdk1 and MAPK activity. As shown in Fig. 8B, MAPK activity was substantially reduced by all tested GDC-0994 concentrations (9.0, -4.0 and -4.4% of the control in oocytes treated with 50, 100 and 200 μM GDC-0994, respectively). The concentrations of 100 and 200 μM reduced MBP phosphorylation to the value which was even lower than the value measured in GV stage oocytes (hence the minus sign).

The western blot results showed that the level of phosphorylated MAPK declined in a concentration-dependent manner with no phosphorylated forms present in the oocytes treated with 200 μM GDC-0994 (Fig. 8A). Notably, phosphorylation level of MAPK did not always

correspond with its activity. For example, phosphorylated forms of MAPK were detected in the 100 μM-treated sample, although the MAPK activity was completely inhibited as demonstrated by the absence of phosphorylation of its downstream targets, p90/RSK and MBP.

All tested GDC-0994 concentrations reduced also Cdk1 activity (measured by phosphorylation of histone H1), although 50 μM just slightly (77.3, 0.3 and -1.4% of the control in oocytes treated with 50, 100 and 200 μM GDC-0994, respectively) and none of them induced cellular stress response as demonstrated by no change in P-eIF2α level when compared to the control (Fig. 8B, C).

In the view of these results, GDC-0994 concentration of 50 μM was chosen for further experiments.

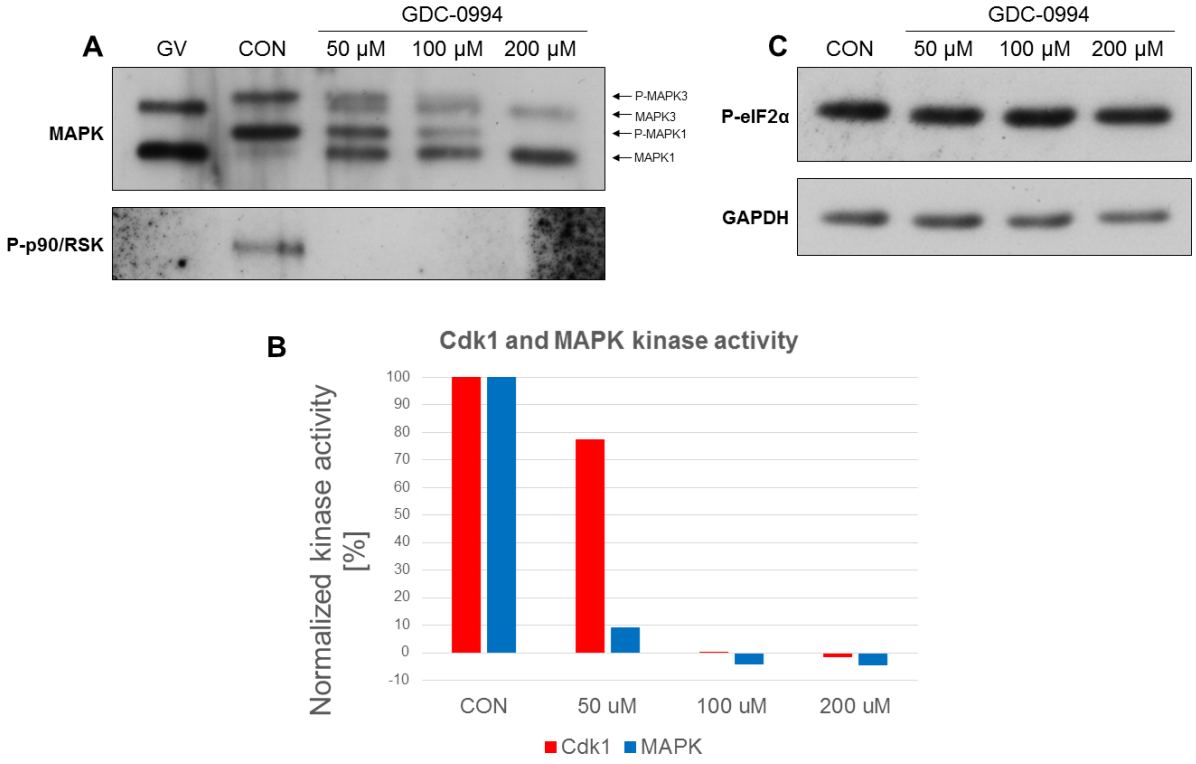

Fig. 8. Effect of GDC-0994 on MAPK phosphorylation, MAPK and Cdk1 activity and eIF2α phosphorylation in mouse oocytes.

Oocytes were cultivated for 7.5 hours in the medium containing 50, 100 or 200 μM of GDC-0994.
A: Western blot results showing the level of both phosphorylated and unphosphorylated forms of MAPK and the level of P-p90/RSK (representing MAPK activity). n = 10 oocytes per sample.
B: *In vitro* kinase assay results showing Cdk1 and MAPK kinase activities reduced by the activities measured in the GV sample and normalized to the activity of control sample. n = 5 oocytes per sample.
C: Western blot results showing the level of P-eIF2α. Glyceraldehyde-3-phosphate dehydrogenase (GAPDH) was used as a loading control. n = 45 oocytes per sample.
CON, control oocytes; GV, germinal vesicle; P, phospho.

5.3 GDC-0994 treatment causes delay of GVBD and prevents MI spindle assembly

It has been reported that oocytes with no MAPK activity progress through meiosis normally, the only major problem being the occurence of spontaneous activation instead of metaphase II arrest (Hashimoto 1996; Verlhac *et al*. 1996; Tong *et al*. 2003). However, no studies using GDC-0994 to inhibit MAPK activity in mouse oocytes have been published yet.

To evaluate the effect of GDC-0994-induced MAPK inhibition on meiosis progression, mouse oocytes were cultured in the medium containing 50 μM GDC-0994 or in the inhibitor-free medium (control group) for 20 hours and GVBD and first polar body extrusion rates were scored at multiple time points.

As shown in Fig. 9A, the GVBD of GDC-0994-treated oocytes was significantly delayed as compared to control group. At 70 min of cultivation 90.2±3.8% (n=155) and 11.2±5.6% (n=245) of untreated and GDC-0994-treated oocytes had undergone GVBD, respectively. The GVBD was not, however, prevented entirely as 97.1±2.8% of GDC-0994-treated oocytes had undergone GVBD when cultured for 7.5 hours (Fig. 9A). The first polar body extrusion rate was scored after 12 hours of cultivation. Whereas 97.5±2.5% (n=47) of control oocytes had extruded the first polar body by that time, none (n=62) of the inhibitor-treated oocytes had done so (Fig. 9B). This result could either mean that the extrusion was delayed or that it was abolished entirely. To distinguish between these two options, oocytes were incubated in the presence of 50 μM GDC-0994 for 20 hours and polar body extrusion rate was then scored. Despite the long cultivation period, none of these oocytes extruded polar body, which was in sharp contrast to 100% of control oocytes having their polar body extruded.

Furthermore, the chromatin and spindle morphology in oocytes cultivated in the presence of 50 μM GDC-0994 for 20 hours was examined. The oocytes were fixed and processed for immunofluorescent staining of microtubules and chromosomes. The control oocytes were arrested at the MII stage with extruded polar body, condensed chromosomes and a spindle of normal shape (Fig. 10A). The chromosomes of GDC-0994-treated oocytes were condensed but not lined up at a metaphase plate corresponding with the absence of an assembled spindle. Two examples of observed GDC-0994-induced phenotypes are shown in Fig. 10B and C.

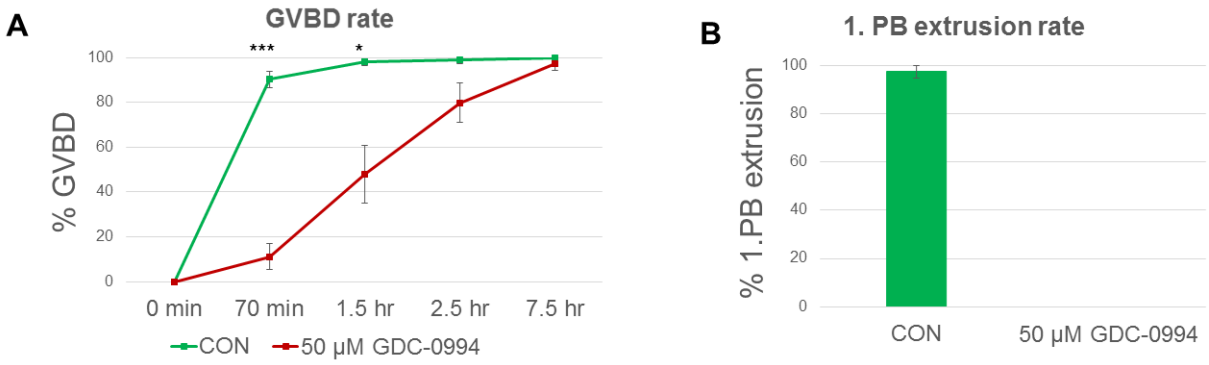

Fig. 9. GDC-0994 treatment causes delay of GVBD and prevents first polar body extrusion.

The graphs showing (A) the GVBD rate (= the percentage of oocytes that underwent GVBD) and (B) the first polar body extrusion rate (= the percentage of oocytes that extruded the first polar body) of the oocytes either treated with 50 μM GDC-0994 or cultivated in the inhibitor-free medium (control oocytes) for (A) 7.5 hours or (B) 12 hours.
A: Data are represented as the means of three independent experiments ± s.d.; asterisk denotes statistically significant differences (Student's t-test; *** means $p < 0.001$; * means $p < 0.05$).
B: Data are represented as the means of two independent experiments ± s.d..
CON, control oocytes; GVBD, germinal vesicle breakdown; PB, polar body.

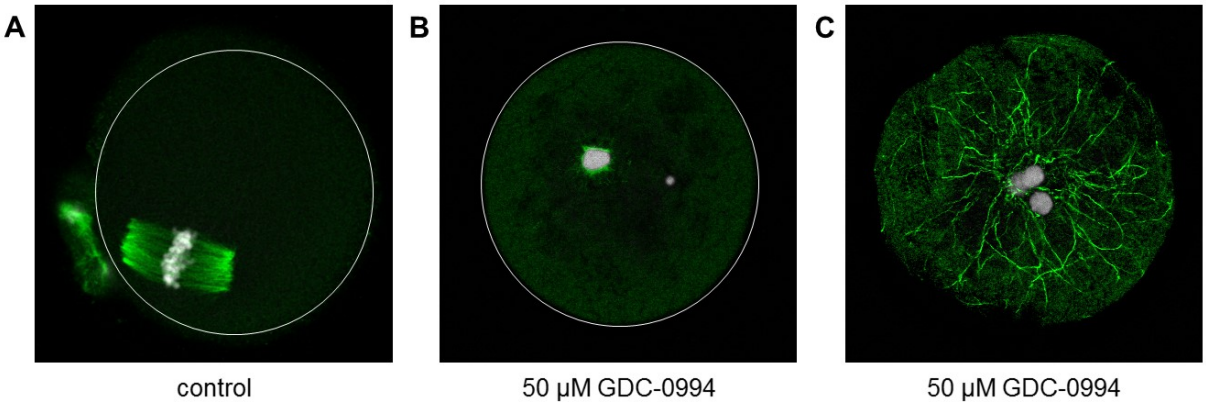

Fig. 10. GDC-0994 treatment causes abnormal chromatin morphology and prevents MI spindle assembly.

Oocytes were cultivated either with (B, C) or without (A) 50 μM GDC-0994 for 20 hours. White line indicates oocyte cortex. Tubulin (green), DAPI (grey). The staining and imaging of the oocytes was done by Markéta Končická.

5.4 Neither cytoplasmic polyadenylation nor translation of cyclin B1 mRNA is affected by MAPK inhibition

To further address the question of an eventual role of MAPK in the regulation of cytoplasmic polyadenylation, the effect of MAPK inhibitor GDC-0994 on the length of cyclin B1 mRNA poly(A) tail in maturing mouse oocytes was evaluated. Moreover, to investigate the possible relationship between cyclin B1 mRNA polyadenylation and delayed GVBD of GDC-0994-treated oocytes, oocytes were sampled according to the time it took them to undergo GVBD.

A group of 150 mouse oocytes was cultured in the medium containing 50 μM GDC-0994 and the oocytes were subsequently divided into four groups according to the following scheme: at 70 minutes the oocytes were examined and a group of oocytes that had undergone GVBD by that time was separated, transferred to a new cultivation well containing 50 μM GDC-0994 and labeled as “GDC-0994, GVBD 70 min”. At 90 minutes of the cultivation the original group of the oocytes (reduced by the group of the oocytes separated at 70 min) was examined again and the oocytes that had undergone GVBD at between 70 and 90 minutes of the cultivation were separated, transferred to another cultivation well containing 50 μM GDC-0994 and labeled as “GDC-0994, GVBD 90 min”. The process was repeated in the same way at 120 minutes generating the third group of oocytes (GDC-0994, GVBD 120 min). The rest of the oocytes that had undergone GVBD no earlier than at 120 minutes of the cultivation was labeled as “GDC-0994, GVBD >120 min”. All oocytes were cultivated in the medium containing 50 μM GDC-0994 for 7.5 hours in total and 98% of them underwent GVBD eventually. Apart from that, samples of fully-grown GV stage oocytes and control oocytes (cultivated in the inhibitor-free medium for 7.5 hours) were also collected.

The poly(A) test assay was employed to assess the level of cyclin B1 mRNA polyadenylation. Cyclin B1 mRNA underwent poly(A) tail elongation during the transition from GV to MI stage (Fig. 11A, lane 1 and 2). No major differences in cyclin B1 poly(A) tail length were observed between GDC-0994-treated and control oocytes as evaluated by position of the smeared band representning the level of polyadenylation (Fig. 11A, lane 2 vs. lane 3 - 6). Moreover, the polyadenylation appeared to be the same in all GDC-0994-treated samples regardless of the GVBD timing (Fig. 11A, lane 3 - 6). However, slight accumulation of the signal in bottom part of the smeared bands in GDC-0994-treated samples (especially in the lanes 3 and 6 of Fig. 11), suggesting that part of the cyclin B1 mRNAs in these samples was not polyadenylated, could not be neglected.

To verify whether MAPK activity was indeed inhibited, the level of P-p90/RSK was examined by western blotting. It appeared that P-p90/RSK was present in the control sample only but

once the X-ray film was exposed to the western blot membrane for a longer time, a faint band was detected also in the GDC-0994-treated sample (Fig. 11B, lane 3) implying that MAPK was strongly, yet not completely inhibited.

As polyadenylation of cyclin B1 mRNA is required for its translation, the amount of cyclin B1 protein was examined at the beginning (fully-grown GV stage oocytes) and at the end of the cultivation. As shown in Fig. 11B, the amount of cyclin B1 in GV oocytes was low (Fig. 11B, lane 1), but it accumulated throughout the maturation reaching the same level in control and GDC-0994-treated oocytes at the end of cultivation (Fig. 11B, lane 2 and 3).

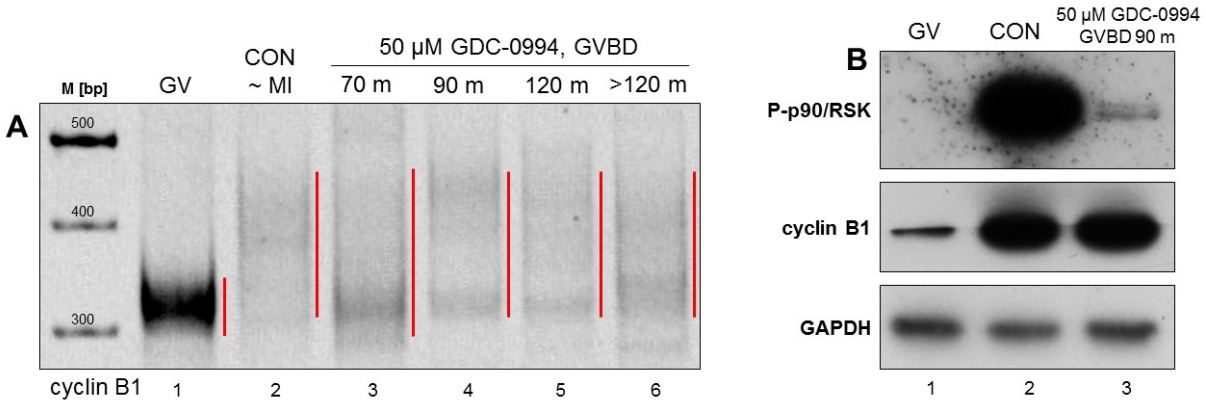

Fig. 11. MAPK inhibition impairs neither polyadenylation nor translation of cyclin B1 mRNA.

Oocytes were cultivated for 7.5 hours in the medium containing 50 µM GDC-0994 or in the inhibitor-free medium (control oocytes, corresponding to MI stage). The oocytes treated with GDC-0994 were divided into four groups (70 m, 90 m, 120 m, >120 m) according to the GVBD timing.

A: PAT assay results showing the effect of 50 µM GDC-0994 on cytoplasmic polyadenylation of cyclin B1 mRNA. The polyadenylation is highlighted by red lines next to each lane. n= 10 oocytes per sample. M, 1 kb DNA Ladder. Lane 1, fully-grown GV stage oocytes; lane 2, control oocytes; lane 3 - 6, oocytes cultivated in the medium containing 50 µM GDC-0994 that had undergone GVBD not later than at 70, 90, 120 min and later than at 120 min of cultivation, respectively.

B: Western blot results showing the level of P-p90/RSK (representing MAPK activity) and cyclin B1. GAPDH was used as a loading control. n = 30 oocytes per sample. Lane 1, fully-grown GV stage oocytes; lane 2, control oocytes; lane 3, oocytes cultivated in the medium containing 50 µM GDC-0994 that had undergone GVBD at between 70 and 90 min of cultivation.

CON, control oocytes; GV, germinal vesicle; GVBD, germinal vesicle breakdown; MI, metaphase I.

5.5 Cyclin B1 mRNA poly(A) tail is elongated during maturation of mouse oocytes despite MAPK and Cdk1 inhibition

As shown in previous sections, GDC-0994 at 50 μM concentration was not sufficient for complete inhibition of MAPK activity. Therefore, the effect of 200 μM GDC-0994 on cyclin B1 mRNA polyadenylation was examined, despite the fact that at such concentration GDC-0994 inhibited also Cdk1 activity.

Oocytes of the control group were cultivated in the inhibitor-free medium. At 80 minutes of cultivation, the oocytes containing intact germinal vesicle (i.e. they had not undergone GVBD) were discarded and the remaining oocytes were cultivated further for up to 12 hours in total. The samples for western blotting, *in vitro* kinase assay and PAT assay were collected at the beginning of maturation (fully-grown GV stage), at 80 minutes (GVBD stage), 7.5 hours (MI stage) and 12 hours (MII stage).

In control group, MAPK was not phosphorylated in the sample of GVBD oocytes (Fig. 12A, lane 2) suggesting that MAPK was not active in this sample, whereas the poly(A) tail of cyclin B1 mRNA was already elongated and its elongation progressed gradually until the MII stage (Fig. 12B, lane 2). The *in vitro* kinase assay results showed that at GVBD and MI stage, Cdk1 activity increased almost 7-fold and 16-fold, respectively, as compared to the GV stage, and subsequently decreased during the MI-MII transition (Fig. 12C). The level of MBP phosphorylation increased slightly (1.5-fold) at GVBD despite the absence of active MAPK (Fig. 12D and Fig. 12A, lane 2). This minor phosphorylation of MBP in the absence of MAPK activity could be explained by the substantial increase of Cdk1 activity at GVBD. Although MBP is mainly phosphorylated by MAPK, it can also be phosphorylated to a small extent by Cdk1 as seen when the *in vitro* kinase assay is performed using a purified active Cdk1 as the only source of kinase activity (Kubelka, unpublished results). The 6.5-fold increase of MAPK activity at the MI stage corresponded with the mobility shift of all MAPK protein to its slow migrating phosphorylated form on the western blot membrane (Fig. 12D and Fig. 12A, lane 3).

In the contrary, the oocytes cultivated in the presence of 200 μM GDC-0994, as well as those cultivated in the presence of IBMX (serving as a negative control), remained arrested in the GV stage. This observation was not unexpected as Cdk1 activity, which is essential for meiosis resumption, was completely inhibited (Fig. 12C). Accordingly, MAPK had not been phosphorylated, thus remained inactive and the poly(A) tail of cyclin B1 mRNA was not elongated throughout the 12-hour cultivation (Fig. 12A, lane 4 and 8; Fig. 12B, lane 4 and 8).

In order to overcome the GV stage arrest which occured when 200 μM GDC-0994 was added at the beginning of maturation, oocytes of the third experimental group were allowed to undergo GVBD in the inhibitor-free medium and were subsequently transferred to the medium

containing 200 μM GDC-0994. None of the oocytes had extruded the first polar body by the end of cultivation. As shown in Fig. 12A, lane 5 and 9, only the unphosphorylated forms of MAPK were present in the samples of oocytes treated with 200 μM GDC-0994 after GVBD. The activity of both MAPK and Cdk1 measured as phosphorylation of their substrates started to decrease slowly after the GDC-0994 addition and reached (in case of MAPK, Fig. 12D) or almost reached (in case of Cdk1, Fig. 12C) the GV activity level after 12 hours of cultivation. However, despite the inhibition of both MAPK and Cdk1 activity, the length of cyclin B1 mRNA poly(A) tail increased progressively until the end of cultivation (Fig. 12A, lane 5 and 9). This result further supports the notion that MAPK is not involved in the regulation of cyclin B1 mRNA polyadenylation.

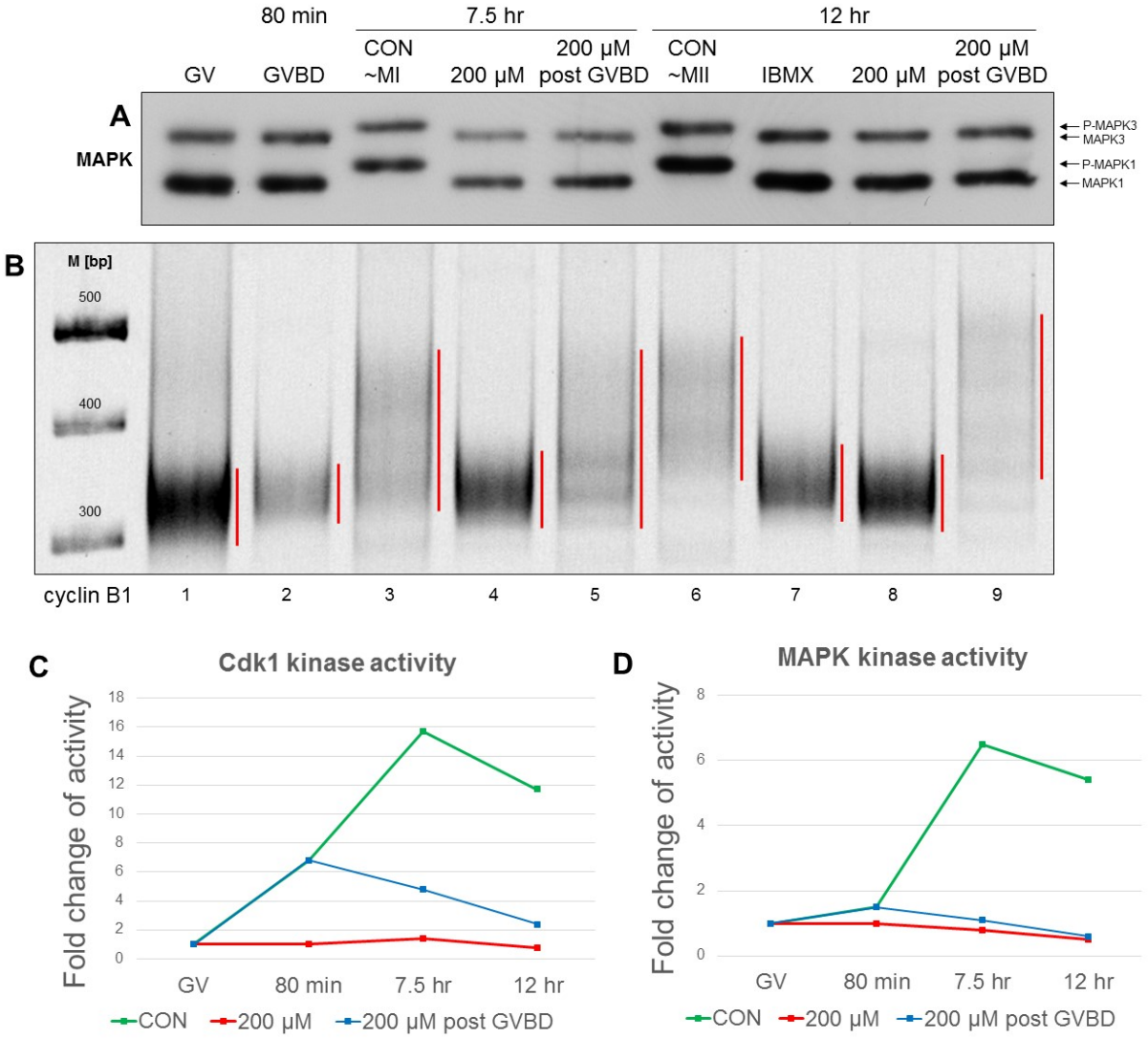

Fig. 12. Cyclin B1 mRNA poly(A) tail is elongated during maturation of mouse oocytes despite MAPK and Cdk1 inhibition.

Four groups of oocytes were analysed in this experiment: I) control oocytes; sample collection at 0 (GV, lane 1), 80 min (GVBD, lane 2), 7.5 hr (MI, lane 3) and 12 hr (MII, lane 6); II) oocytes cultivated in the presence of 200 μM GDC-0994; sample collection at 7.5 hr (lane 4) and 12 hr (lane 8); III) oocytes transferred to the medium containing 200 μM GDC-0994 at the GVBD stage; sample collection at 7.5 hr (lane 5) and 12 hr (lane 9); IV) oocytes cultivated in the medium containing IBMX for 12 hr (lane 7).
A: Western blot results showing the level of both phosphorylated and unphosphorylated forms of MAPK. n = 10 oocytes per sample.
B: PAT assay results showing the level of cyclin B1 mRNA polyadenylation. The polyadenylation is highlighted by red lines next to each lane. n= 10 oocytes per sample. M, 1 kb DNA Ladder.
C, **D**: *In vitro* kinase assay results showing (C) Cdk1 and (D) MAPK kinase activities. n = 5 oocytes per sample. The value of the activity obtained for the GV sample was set as 1.
CON, control oocytes; GV, germinal vesicle; GVBD, germinal vesicle breakdown; IBMX, 3-isobutyl-1-methylxanthine; MI/II, metaphase I/II; P, phospho.

5.6 MAPK inhibition results in reduced polyadenylation of cyclin B1 mRNA in cumulus-enclosed mouse oocytes

Mouse oocytes isolated from the ovary are surrounded by several layers of cumulus cells. The cumulus cells are usually removed and denuded oocytes are cultivated further. The advantage of cumulus cells removal is that meiotic resumption manifested by germinal vesicle breakdown and the first polar body extrusion are clearly visible when oocytes are denuded, which is useful when examining the maturation stage of oocytes during cultivation. Moreover, the attachment of cumulus cells to fully-grown oocyte is very loose and they tend to detach even when manipulated very carefully. Therefore it is much easier to obtain a group of denuded mouse oocytes than a group of cumulus-enclosed oocytes. Importantly, there is no difference in the maturation rate of denuded and cumulus-enclosed mouse oocytes when cultured *in vitro* (Leonardsen *et al*. 2000; Su *et al*. 2001).

It has been proposed that cumulus cells surrounding mouse oocyte play role in regulation of maternal mRNAs translation. In particular, the accumulation of TPX2 protein during meiotic maturation of mouse oocytes is markedly reduced in denuded oocytes as compared to the oocytes matured in association with cumulus cells (Chen *et al*. 2013). Importantly, translation of tpx2 mRNA is driven by cytoplasmic polyadenylation of this transcript during the transition from the GV to MI stage (Sha *et al*. 2016). Based of these findings, an experiment using cumulus-enclosed mouse oocytes was conducted in order to verify whether the presence of cumulus cells influences the effect of MAPK inhibition on cytoplasmic polyadenylation of cyclin B1 mRNA.

The cumulus-enclosed oocytes (CEOs) were cultivated in the medium containing 10 or 50 μM GDC-0994 or in the inhibitor-free medium for 7.5 hours. At the end of cultivation, the cumulus cells were removed and samples for western blotting, *in vitro* kinase assay and PAT assay were collected. The GVBD rate of CEOs examined at the end of cultivation was 100% (n=35), 96% (n=28) and 22% (n=41) for the control, 10 μM and 50 μM GDC-0994-treated oocytes, respectively (Fig. 13A).

The kinase activities of both Cdk1 and MAPK were assessed by the *in vitro* kinase assay. Interestingly, stronger inhibition of both kinases was observed when 50 μM GDC-0994 was applied to CEOs as compared to denuded oocytes (DOs). Both MAPK and Cdk1 activities were inhibited completely in CEOs treated with 50 μM GDC-0994 (Fig. 13B). Accordingly, phosphorylated forms of MAPK on the western blot membrane were almost undetectable (Fig. 13C, lane 4). The effect of 10 μM GDC-0994 on the kinase activity in CEOs (16.1% and 69.4% of the control for MAPK and Cdk1, respectively) was comparable to the effect of 50 μM

GDC-0994 in DOs (9% and 77.3% of the control for MAPK and Cdk1, respectively) (Fig. 13B for CEOs and Fig. 8B for DOs).

The most interesting was the result of PAT assay. The treatment of CEOs with 10 μM GDC-0994 resulted in a clear reduction of cyclin B1 mRNA poly(A) tail length (Fig. 13D, lane 3). This finding is in sharp contrast to the situation observed in denuded oocytes, where polyadenylation was unchanged despite even stronger inhibition of MAPK activity (Fig. 11A).

These results suggest that MAPK signaling in the cumulus cells might play a role in the regulation of cytoplasmic polyadenylation of mRNAs stored in the oocyte.

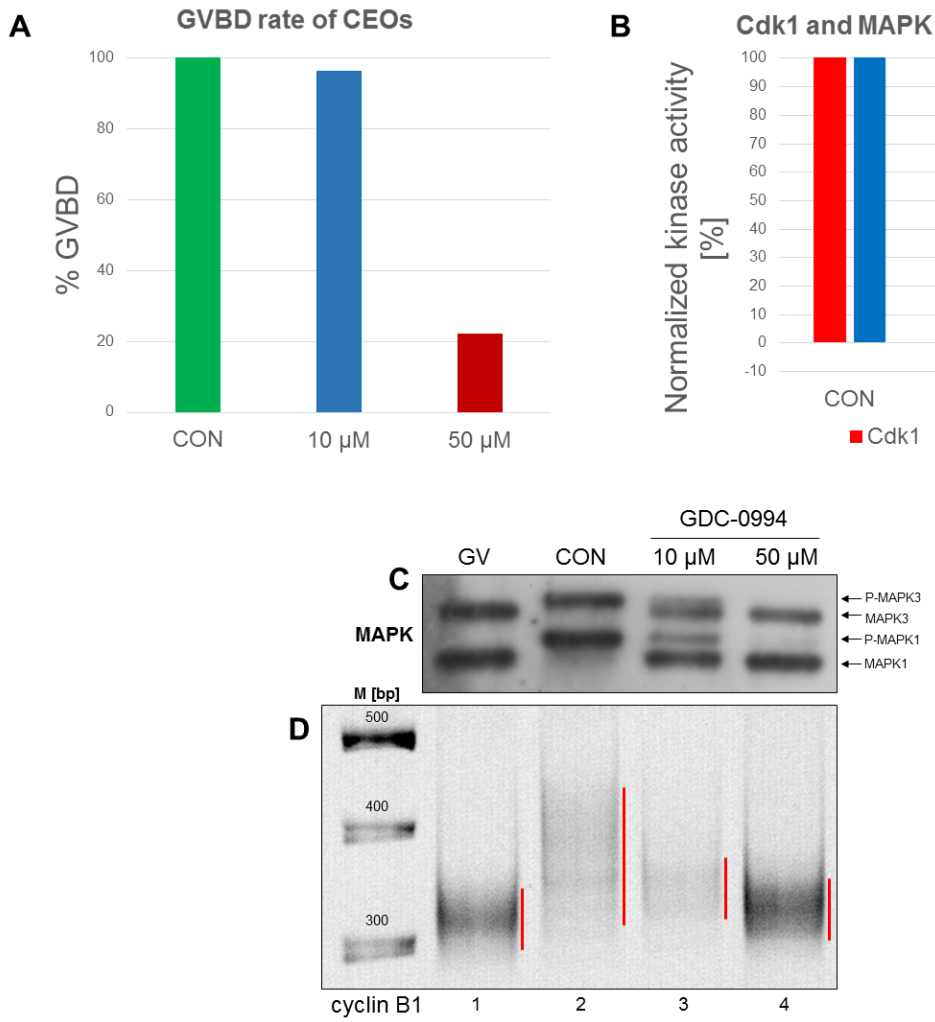

Fig. 13. MAPK inhibition results in reduced level of cyclin B1 mRNA polyadenylation in cumulus-enclosed mouse oocytes.

Cumulus-enclosed mouse oocytes were cutivated for 7.5 hours in the medium containing 10 or 50 μM GDC-0994 or in the inhibitor-free medium (control oocytes).
A: The graph showing the GVBD rate of CEOs.
B: *In vitro* kinase assay results showing Cdk1 and MAPK kinase activities reduced by the activities measured in GV sample and normalized to the activity of control sample. n = 5 oocytes per sample.
C: Western blot results showing the level of phosphorylated and unphosphorylated forms of MAPK. n = 10 oocytes per sample.
D: PAT assay results showing the level of cyclin B1 mRNA polyadenylation. The polyadenylation is highlighted by red lines next to each lane. n = 10 oocytes per sample. M, 1 kb DNA Ladder.
CEO, cumulus-enclosed oocyte; CON, control oocytes; GV, germinal vesicle; GVBD, germinal vesicle breakdown; P, phospho.

5.7 MAPK activation correlates with cyclin B1 mRNA polyadenylation during meiotic maturation of porcine oocytes

As in mouse oocytes, both MAPK activation and cyclin B1 mRNA polyadenylation have been reported to occur in maturing porcine oocytes (Inoue *et al*. 1995; Zhang *et al*. 2010a), yet the time sequence of these events has not yet been investigated. The same question as in the case of mouse oocytes was addressed, i.e. whether cytoplasmic polyadenylation of cyclin B1 mRNA depends on MAPK activation during maturation of porcine oocytes.

It is important to point out that porcine oocytes have been cultured in the presence of cumulus cells unless stated otherwise. There are two reasons for this. First, in contrast to mouse oocytes, porcine oocytes progress through meiotic maturation with higher rate and in better shape when cultured with cumulus cells when compared to denuded ones. Second, it is technically very difficult to remove cumulus cells from GV stage porcine oocytes as they are attached to the oocyte tightly.

At first, I examined the cyclin B1 mRNA polyadenylation status in maturing porcine oocytes. The samples for PAT assay were collected at multiple time points during 45 hour cultivation. The collection interval was shorter around the time of GVBD (appx. after 20 hours of maturation). As shown in Fig. 14, the polyadenylation of cyclin B1 mRNA was first visible in the extract of oocytes cultivated for 21 hours. At this time, 73% of the evaluated oocytes had undergone GVBD. At 18 hours of maturation the polyadenylation was not detected, yet 40% of the evaluated oocytes had undergone GVBD by that time. The cyclin B1 mRNA poly(A) tail was elongated gradually from 21 hours up to 28 hours of maturation and remained long until the end of cultivation.

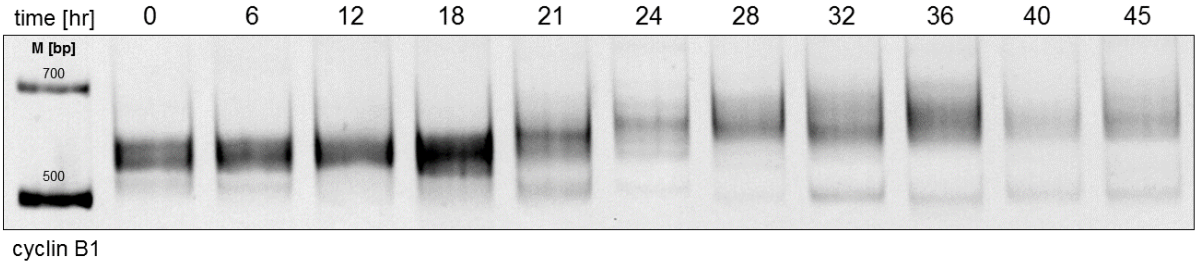

Fig. 14. Cyclin B1 mRNA is polyadenylated after 21 hours of porcine oocyte maturation.

PAT assay results showing the level of cyclin B1 mRNA polyadenylation during maturation of porcine oocytes. n= 10 oocytes per sample. M, 1 kb DNA Ladder.

Subsequently, the time sequence of MAPK activation and cyclin B1 mRNA polyadenylation was investigated. Porcine oocytes were cultivated and samples for western blotting and PAT assay were collected at the beginning (GV stage oocytes) and after 21, 28 and 46 hours of maturation. All elucidated aspects, i.e. activating phosphorylation of MAPK, MAPK activity measured as p90/RSK phosphorylation, amount of cyclin B1 protein and cyclin B1 mRNA polyadenylation, were first detected in the sample of oocytes collected at 21 hours of maturation, when 65% of oocytes had undergone GVBD (Fig. 15). On the basis of this result it cannot be concluded whether MAPK activation precedes cyclin B1 mRNA polyadenylation.

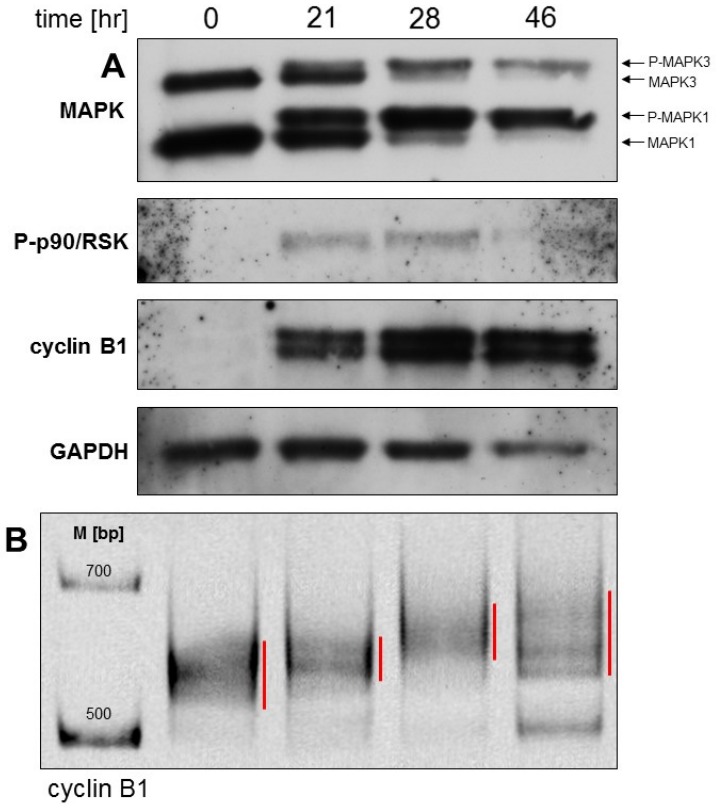

Fig. 15. MAPK is activated, cyclin B1 protein accumulated and cyclin B1 mRNA polyadenylated during porcine oocyte maturation.

Porcine oocytes were cultivated and samples were collected at the beginning (GV stage oocytes) and after 21, 28 and 46 hours of maturation.
A: Western blot results showing the level of both phosphorylated and unphosphorylated forms of MAPK, the level of P-p90/RSK (representing MAPK activity) and the level of cyclin B1. GAPDH was used as a loading control. n = 30 oocytes per sample. P, phospho.
B: PAT assay results showing the level of cyclin B1 mRNA polyadenylation. The polyadenylation is highlighted by red lines next to each lane. n = 10 oocytes per sample. M, 1 kb DNA Ladder.

5.8 Effect of GDC-0994 treatment on cyclin B1 mRNA polyadenylation and meiotic maturation of porcine oocytes

I further aimed to evaluate the effect of MAPK inhibition on cyclin B1 mRNA polyadenylation and meiotic maturation of both cumulus-enclosed and denuded porcine oocytes.

Cumulus-enclosed oocytes were cultivated in the presence of 10 or 25 μM GDC-0994 for 45 hours and samples for *in vitro* kinase assay, western blotting and PAT assay were collected. The results of *in vitro* kinase assay showed that both MAPK and Cdk1 kinase activities were completely inhibited (data not shown). In accordance with the complete Cdk1 inhibition, all GDC-0994-treated oocytes remained arrested in the GV stage and did not resume meiosis. The absence of cyclin B1 mRNA poly(A) tail elongation, as well as the absence of phosphorylated MAPK forms in the GDC-0994-treated samples, was the consequence of impaired maturation (Fig. 16). In further experiments, lower concentrations of GDC-0994 have to be tested in order to find optimal conditions leading to MAPK inhibition, yet not affecting the Cdk1 activity.

To evaluate the effect of GDC-0994 treatment in denuded porcine oocytes, cumulus cells were removed before maturation and oocytes were cultivated in the presence of 25 μM GDC-0994 for 28 hours. Due to technical reasons it was not possible to examine the maturation stages of the oocytes at the end of the cultivation, which made the interpretation of results complicated. Both western blot and *in vitro* kinase assay results showed that MAPK activity was completely inhibited in the GDC-0994-treated oocytes (Fig. 17A, C). The Cdk1 activity, however, was 2-fold higher in treated oocytes as compared to control oocytes, which was surprising. Moreover, the poly(A) tail of cyclin B1 mRNA was elongated neither in treated oocytes nor in control oocytes (Fig. 17B).

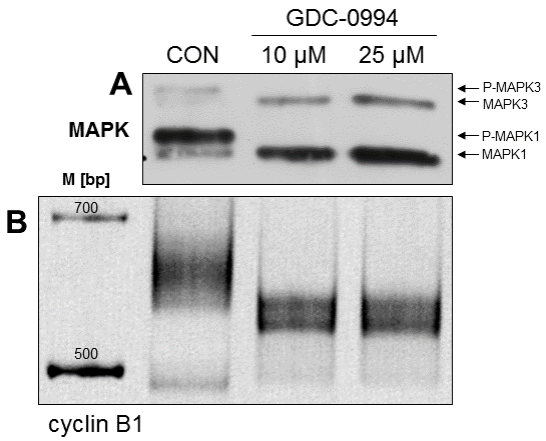

Fig. 16. The GDC-0994 concentration of 10 μM blocks meiotic maturation of cumulus-enclosed porcine oocytes.

Cumulus-enclosed porcine oocytes were cutivated for 45 hours in the medium containing 10 or 25 μM GDC-0994 or in the inhibitor-free medium (control oocytes).
A: Western blot results showing the level of both phosphorylated and unphosphorylated forms of MAPK. n = 10 oocytes per sample.
B: PAT assay results showing the level of cyclin B1 mRNA polyadenylation. n = 10 oocytes per sample. M, 1 kb DNA Ladder. CON, control oocytes; P, phospho.

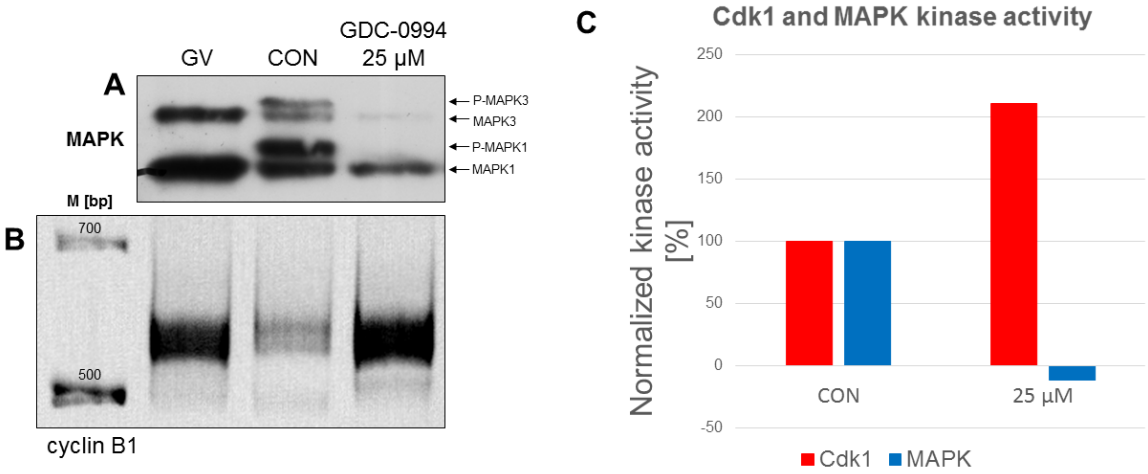

Fig. 17. The effect of GDC-0994 on MAPK phosphorylation, cyclin B1 mRNA polyadenylation and both MAPK and Cdk1 activities in denuded porcine oocytes.

Denuded porcine oocytes were cutivated for 28 hours in the medium containing 25 μM GDC-0994 or in the inhibitor-free medium (control oocytes).
A: Western blot results showing the level of both phosphorylated and unphosphorylated forms of MAPK. n = 10 oocytes per sample.
B: PAT assay results showing the level of cyclin B1 mRNA polyadenylation. n = 10 oocytes per sample. M, 1 kb DNA Ladder.
C: *In vitro* kinase assay results showing Cdk1 and MAPK kinase activities reduced by the activities measured in GV sample and normalized to the activity of control sample. n = 5 oocytes per sample. CON, control oocytes; GV, germinal vesicle; P, phospho.

6. DISCUSSION

A regulated shortening and elongation of mRNA poly(A) tail is a mechanism enabling temporal regulation of translation widely used in maturing oocytes. Maternal mRNAs possessing short poly(A) tails are stored in the oocyte cytoplasm in translationally repressed state. Later on, precisely timed elongation of the poly(A) tail destines mRNA for translation and the synthesized proteins then drive meiotic progression of the oocyte. The aim of this thesis is to examine whether mitogen-activated protein kinase (MAPK) is involved in regulation of maternal mRNAs poly(A) tail length in maturing mouse and porcine oocytes.

Firstly, I have demonstrated that polyadenylation of cyclin B1 mRNA precedes MAPK activation in maturing mouse oocytes, implying that MAPK is not required for activation of cytoplasmic polyadenylation. This result is consistent with the fact that Mos kinase, the kinase acting upstream of MAPK, is absent in the GV-arrested oocytes and its synthesis depends on cytoplasmic polyadenylation of mos mRNA (Gebauer *et al*. 1994, Verlhac *et al*. 1996). Since MAPK acts downstream of Mos, it is implausible that MAPK activates cytoplasmic polyadenylation and subsequent translation of mos mRNA. However, I cannot rule out a possibility that there are several mechanisms, each of them regulating cytoplasmic polyadenylation of a different subset of maternal mRNAs. If this were the case, mos mRNA could be polyadenylated in MAPK-independent manner but at the same time, MAPK could be responsible for polyadenylation of some other mRNAs later during maturation. Alternatively, MAPK could be transiently activated early during maturation, independently of Mos expression, as has been demonstrated in *Xenopus* oocytes (Keady *et al*. 2007). This early MAPK activation could then be responsible for mos and cyclin B1 mRNA polyadenylation. It would be interesting to examine the timing of mos and cyclin B1 mRNA polyadenylation in maturing mouse oocytes to determine whether polyadenylation of both mRNAs occurs simultaneously and is thus likely to be regulated by the same signaling pathway. In addition, analysis of oocyte samples collected in short time intervals covering the early period of maturation should be performed to detect the possible early and transient MAPK activation. Last but not least, inactive form of Mos kinase could be present in GV-arrested oocytes in very low amounts and could, in response to an unknown signal, activate MAPK which would in turn drive the polyadenylation of mos mRNA and subsequent accumulation of Mos protein. This scenario provides a possible explanation of how MAPK could regulate synthesis of its upstream kinase. Nevertheless, there is more evidence for Mos being absent (Verlhac *et al*. 1996, Bernhardt *et al*. 2011, Kong *et al*. 2012) than being present in low amounts (Paules *et al*. 1989) in GV-arrested mouse oocytes. Moreover, Mos kinase activity is regulated at the level of Mos synthesis and degradation rather then by post-translational modifications. For these reasons, the last scenario is implausible.

To further investigate a possible role of MAPK in regulation of cytoplasmic polyadenylation I aimed to evaluate the effect of MAPK inhibition on polyadenylation of cyclin B1 mRNA. I have used commercially available MAPK inhibitor called GDC-0994. The mechanism of action of this inhibitor is not specified by the manufacturer. I have shown that MAPK inhibition by GDC-0994 is reversible (data not shown) and that GDC-0994 abolishes MAPK kinase activity as well as reduces activating MAPK phosphorylation carried out by MEK. It can be speculated whether the latter effect is caused by the nonspecific effect of the inhibitor on MEK or by some conformational change of MEK phosphorylation or binding site within MAPK protein. When used at high concentrations, the inhibitor abolishes both MAPK and Cdk1 kinase activities. The concentration of 50 μM was chosen for further experiments as it reduced MAPK activity markedly whereas Cdk1 activity just slightly. However, even a slight reduction of Cdk1 activity can negatively affect meiotic progression and complicates interpretation of the obtained results. For future experiments it would probably be worth testing another MAPK inhibitor.

Mouse oocytes treated with 50 μM of GDC-0994 failed to assemble the meiotic spindle, extrude the first polar body and they resumed meiosis with a significant delay as compared to the oocytes cultured in the inhibitor-free medium. This phenotype was surprising, as it has been shown several times that MAPK activity is not required for the oocytes to undergo GVBD and to complete the first meiotic division (Choi *et al*. 1996, Hashimoto 1996, Verlhac *et al*. 1996, Tong *et al*. 2003, Zhang *et al*. 2015, Yu *et al*. 2016). For this reason it can be assumed that the observed phenotype results from the partial Cdk1 inhibition. Cdk1 kinase activity increases gradually in maturing oocytes reaching its maximum at the time of the first meiotic spindle formation (Verlhac *et al*. 1994). It can be speculated that the reduced Cdk1 activity in GDC-0994-treated oocytes is sufficient for meiotic resumption but not high enough for further meiotic progression. Alternatively, the inhibitor might non-specifically inhibit some other kinases important for meiotic spindle assembly.

The inhibition of MAPK by GDC-0994 did not have a major effect on the poly(A) tail length of cyclin B1 mRNA irrespective of the GVBD timing. A slight enrichment of cyclin B1 mRNAs possessing a short poly(A) tail was observed in the inhibitor-treated oocyte samples. Nevertheless, the expression of cyclin B1 protein was not affected. Moreover, the poly(A) tail length of cyclin B1 mRNA increased progressively even when the GVBD stage oocytes were transferred to the medium containing high inhibitor concentration. It should be noted that at the time of oocyte transfer MAPK had not yet been activated, ruling out the possibility that MAPK could have triggered polyadenylation before the inhibitor was added. In addition, the polyadenylation of cyclin B1 mRNA has already been detected in the GVBD stage oocytes, confirming my previous observation that polyadenylation of cyclin B1 mRNA precedes MAPK activation.

My results are in sharp contrast with the conclusion made by Sha *et al*. (2016) who have proposed that MAPK inhibition impairs cyclin B1 mRNA polyadenylation in maturing mouse oocytes. However, the data presented in this publication does not prove this statement. First of all, the presented picture of poly(A) tail assay does not actually show that MAPK inhibition blocks polyadenylation of cyclin B1 mRNA (Fig. 18). The smeared and faint signal in the GV stage oocyte sample does not correspond to the fact that cyclin B1 mRNAs possess short poly(A) tail in the GV-arrested oocytes and this should yield a compact band of a relatively small size. Moreover, cyclin B1 mRNA is polyadenylated in both control and inhibitor-treated samples. Second, no information on the maturation rate of the inhibitor-treated oocytes is provided. Delayed maturation could result in an enrichment of mRNAs with relatively short poly(A) tails (Fig. 18, blue arrowhead) as well as in decreased amount of cyclin B1 protein in the inhibitor-treated sample. Third, even though most of the results presented in the above-mentioned publication were obtained using MAPK-deficient oocytes (*Mapk*$^{-/-}$), the experiments addressing the role of MAPK in cytoplasmic polyadenylation were conducted using wild-type oocytes treated with an inhibitor of MEK (U0126), the kinase acting upstream of MAPK. It would be interesting to see whether polyadenylation of cyclin B1 mRNA in maturing *Mapk*$^{-/-}$ oocytes is reduced when compared to wild-type oocytes. Fourth, oocytes isolated from C57B6 mice were used in this study, whereas CD1 mice were used for the experiments presented in my thesis. However, I do not think that molecular mechanisms controlling such an important process as is cytoplasmic polyadenylation differ among different mouse strains. In future I would like to repeat my experiments using the same inhibitor as was used in this study.

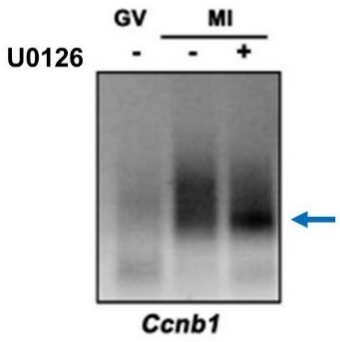

Fig. 18. Effect of MAPK inhibition on cyclin B1 mRNA polyadenylation in mouse oocytes.

The result of poly(A) tail assay taken from Sha *et al*. (2016) showing the level of cyclin B1 mRNA polyadenylation in mouse oocytes cultured either with or without MEK inhibitor (U0126). Blue arrowhead shows an enrichment of mRNAs with relatively short poly(A) tails in the inhibitor-treated sample.

It has been shown that the presence of cumulus cells can affect protein synthesis in mouse oocytes (Chen *et al*. 2013). For this reason I have aimed to evaluate the effect of MAPK inhibition on cytoplasmic polyadenylation in cumulus-enclosed mouse oocytes. Indeed, when cultured in the presence of both, cumulus cells and MAPK inhibitor, polyadenylation of cyclin B1 mRNA in oocytes was reduced. It is tempting to speculate that active MAPK in the cumulus cells triggers some signaling pathway in the oocyte, which then promotes polyadenylation of maternal mRNAs. At the same time, polyadenylation does not depend on the presence of cumulus cells as it is not impaired in denuded oocytes.

According to a hypothetical model that I propose, the presence of cumulus cells prevents polyadenylation of mRNAs stored in the oocyte unless MAPK in the cumulus cells is activated. Either when MAPK is activated in the cumulus cells or when the cumulus cells are removed, polyadenylation is triggered through an unknown signaling mechanism acting in the oocyte. It has already been demonstrated that translation of specific maternal mRNAs, namely tpx2 and dazl mRNAs, increases in the oocytes cultured with cumulus cells in response to EGF-like growth factors added to the cultivation medium (Chen *et al*. 2013). Notably, translation of both mentioned mRNAs is controlled by cytoplasmic polyadenylation (Chen *et* al. 2011, Sha *et al*. 2016). EGF-like growth factors act through EGF receptors present in the plasma membrane of cumulus cells and the signal generated by cumulus cells triggers activation of PI(3)K-AKT-mTOR pathway within the oocyte (Chen *et al*. 2013). A connection between mTOR signaling and cytoplasmic polyadenylation has not yet been shown, however, another mTOR downstream target, protein kinase C zeta type, is involved in the control of mos mRNA polyadenylation in *Xenopus* oocytes (Sarkissian *et al*. 2004).

However, no conclusions can be made at this point. First of all, I need to repeat my experiments more times to verify the observations I have made. Second, it is necessary to evaluate the activity of MAPK in the cumulus cells as the proposed model could only be valid in the case when MAPK is active in the cumulus cells cultured under normal conditions (without MAPK inhibitor). Third, I have to rule out the possibility that reduced polyadenylation results from delayed maturation of the inhibitor-treated oocytes. At the time of sample collection, almost all oocytes have undergone GVBD. I do not know, however, whether they underwent GVBD soon after beginning of the cultivation or shortly before sample collection. Moreover, the capacity of the cumulus-enclosed mouse oocytes treated with MAPK inhibitor to complete meiotic maturation and arrest at the MII stage has to be examined.

In the last part of my thesis I aimed to investigate a relationship between MAPK activity and cytoplasmic polyadenylation in maturing porcine oocytes. In contrast to mouse oocytes, porcine oocytes do not undergo GVBD and proceed through meiosis when protein synthesis

is blocked (Fulka *et al*. 1986). Clearly, some protein(s) important for meiotic resumption are missing in porcine GV stage oocytes and must be synthesized to induce GVBD. This protein is most likely cyclin B1 or some other protein which can stimulate Cdk1 kinase activity. As in mouse oocytes, the synthesis of cyclin B1 is controlled by cytoplasmic polyadenylation (Zhang *et al*. 2010). If MAPK were involved in activation of cytoplasmic polyadenylation hence synthesis of cyclin B1, I would expect porcine oocytes to not resume meiosis when treated with MAPK inhibitor. Moreover, the synthesis of Mos kinase is also controlled by cytoplasmic poyladenylation in porcine oocytes (Dai *et al*. 2005), which raises the same question regarding the order of mos mRNA polyadenylation and MAPK activation as was discussed above for mouse oocytes.

It is important to keep two unpleasant aspects of porcine oocyte maturation in mind when performing an experiment and interpreting the results. First, porcine oocytes mature not as synchronously as mouse oocytes. Therefore, at every time of the maturation period (except for the very beginning, when oocytes are GV-arrested, and the very end of maturation, when all oocytes have already reached the MII stage), the oocyte population is rather heterogeneous regarding the maturation stage. Moreover, the oocyte cytoplasm contains opaque lipid droplets making it impossible to determine the maturation stage of living oocytes at the moment of sample collection. For these reasons, when a sample is collected, part of the oocytes must be fixed, stained and imaged to estimate the proportion of any particular maturation stage in the sample.

For the reasons mentioned above, it was not possible to examine whether MAPK activation precedes meiotic resumption in porcine oocytes. One way to overcome the heterogenity in the maturation stage within a population of porcine oocytes would be to synchronize the oocytes at the late-diplotene stage before maturation. There are several synchronization protocols employing different mechanisms of meiotic resumption prevention (Somfai and Hirao 2011). Some of them are based on a global inhibition of protein synthesis. However, those shoud be avoided when investigating mechanisms of translational regulation.

Both MAPK activation and cyclin B1 mRNA polyadenylation were detected in the sample of cumulus-enclosed porcine oocytes collected after 21 hours of maturation. Based on this result it cannot be concluded which of these events precedes the other. The experiment will be repeated and samples will be collected at shorter intervals, especially around the time of cyclin B1 mRNA polyadenylation onset. Moreover, several concentrations of MAPK inhibitor were tested to examine the effect of MAPK inhibition on cytoplasmic polyadenylation in maturing cumulus-enclosed porcine oocytes. However, even the lowest tested concentration of 10 μM caused complete inhibition of Cdk1 as well as MAPK kinase activity. Therefore, even

lower concentrations will be tested in order to find such concentration that would reduce MAPK activity only. Since different effects of MAPK inhibition were observed in cumulus-enclosed and denuded mouse oocytes, I aimed to address the same question using denuded porcine oocytes. At the end of the maturation culture, denuded porcine oocytes exhibited unusual shrinked morphology, which complicated the evaluation of their maturation stage. It has been shown, that porcine oocytes deprived of cumulus cells exhibit decreased *in vitro* maturation rate and developmental competence when compared to cumulus-enclosed porcine oocytes (Wongsrikeao *et al*. 2005, Zhang *et al.* 2010b). Moreover, the polyadenylation of cyclin B1 mRNA was impaired even in the denuded oocytes cultivated without MAPK inhibitor. For these reasons, I would suggest to continue the work on my project using the cumulus-enclosed porcine oocytes only.

In summary, it is unlikely, at least in mouse oocytes, that MAPK plays role in activation of cytoplasmic polyadenylation of cyclin B1 mRNA during meiotic maturation. This conclusion raises a question of which kinase(s), if not MAPK, are involved in this process. Based on biochemical studies performed using *Xenopus* oocytes, several kinases have been proposed to participate in CPEB-mediated cytoplasmic polyadenylation (see section 2.3.4). However, molecular mechanisms controlling meiotic resumption of *Xenopus* oocytes differ remarkably from those employed in mammalian oocytes. Therefore, I would rather focus on a potential role of CaMKII which has been shown to phosphorylate CPEB in mouse hippocampal neurons (Atkins *et al*. 2004). Interestingly, CaMKII inhibition did not prevent meiotic resumption but blocked the first polar body extrusion in mouse oocytes (Su and Eppig 2002), resembling the expected phenotype of cyclin B1 synthesis inhibition. It would be interesting to investigate the effect of CaMKII inhibition on cyclin B1 mRNA polyadenylation and translation. Alternatively, *in vitro* screening for kinase phosphorylating CPEB protein used as a substrate could be performed.

7. CONCLUSIONS

The possible role of mitogen-activated protein kinase (MAPK) in regulation of cytoplasmic polyadenylation of cyclin B1 mRNA in maturing mouse and porcine oocytes was investigated in this study. The following conclusions have been made on the basis of the obtained results.

1. MAPK activity is not required for cytoplasmic polyadenylation of cyclin B1 mRNA in mouse oocytes matured in the absence of cumulus cells.

• Polyadenylation of cyclin B1 mRNA was first detected at the time of GVBD when MAPK had not yet been activated.

• Inhibition of MAPK activity impaired neither polydenylation nor translation of cyclin B1 mRNA.

• Not only was polyadenylation of cyclin B1 mRNA preserved, but it increased gradually in maturing oocytes despite the complete inhibition of MAPK activity.

2. MAPK activity in cumulus cells attached to maturing mouse oocytes influences cytoplasmic polyadenylation of cyclin B1 mRNA in the oocytes.

• When oocytes were matured in the presence of cumulus cells, polyadenylation of cyclin B1 mRNA in oocytes was unaffected. However, when matured in the presence of both cumulus cells and MAPK inhibitor, polyadenylation of cyclin B1 mRNA was reduced.

3. Timing of MAPK activation correlates with cyclin B1 mRNA polyadenylation in porcine oocytes matured in the presence of cumulus cells.

• Both MAPK activity and cyclin B1 mRNA polyadenylation were detected at the time of GVBD in oocytes surrounded by cumulus cells.

4. Presence of cumulus cells is required for correct maturation of porcine oocytes.

• Porcine oocytes exhibited unusual morphology and impaired polyadenylation of cyclin B1 mRNA when matured in the absence of cumulus cells.

5. The GDC-0994 compound used in this study has also unspecific effects.

• When used at concentration high enough to completely inhibit MAPK activity, GDC-0994 reduced also Cdk1 activity.

8. REFERENCES

* review article; ** book chapter

Adhikari D, Zheng W, Shen Y, Gorre N, Ning Y, Halet G, Kaldis P, Liu K (2012): Cdk1, but not Cdk2, is the sole Cdk that is essential and sufficient to drive resumption of meiosis in mouse oocytes. Hum. Mol. Genet. 21: 2476-2484.

Atkins CM, Nozaki N, Shigeri Y, Soderling TR (2004): Cytoplasmic polyadenylation element binding protein-dependent protein synthesis is regulated by calcium/calmodulin-dependent protein kinase II. J. Neurosci. 24: 5193-5201.

Bernhardt ML, Kim AM, O'Halloran TV, Woodruff TK (2011): Zinc requirement during meiosis I-meiosis II transition in mouse oocytes is independent of the MOS-MAPK pathway. Biol. Reprod. 84: 526-536.

Cao Q, Richter JD (2002): Dissolution of the maskin-eIF4E complex by cytoplasmic polyadenylation and poly(A)-binding protein controls cyclin B1 mRNA translation and oocyte maturation. EMBO J. 21: 3852-3862.

Charlesworth A, Cox LL, MacNicol AM (2004): Cytoplasmic polyadenylation element (CPE)- and CPE-binding protein (CPEB)-independent mechanisms regulate early class maternal mRNA translational activation in Xenopus oocytes. J. Biol. Chem. 279: 17650-17659.

* Charlesworth A, Meijer HA, de Moor CH (2013): Specificity factors in cytoplasmic polyadenylation. Wiley Interdiscip. Rev.: RNA. 4: 437-461.

Chen J, Melton C, Suh N, Oh JS, Horner K, Xie F, Sette C, Blelloch R, Conti M (2011): Genome-wide analysis of translation reveals a critical role for deleted in azoospermia-like (Dazl) at the oocyte-to-zygote transition. Genes Dev. 25: 755-766.

Chen J, Torcia S, Xie F, Lin CJ, Cakmak H, Franciosi F, Horner K, Onodera C, Song JS, Cedars MI, Ramalho-Santos M, Conti M. (2013): Somatic cells regulate maternal mRNA translation and developmental competence of mouse oocytes. Nat. Cell Biol. 15: 1415-1423.

Choi T, Fukasawa K, Zhou R, Tessarollo L, Borror K, Resau J, Vande Woude GF (1996): The Mos/mitogen-activated protein kinase (MAPK) pathway regulates the size and degradation of the first polar body in maturing mouse oocytes. Proc. Natl. Acad. Sci. U. S. A. 93: 7032-7035.

Dai Y, Newman B, Moor R (2005): Translational regulation of MOS messenger RNA in pig oocytes. Biol. Reprod. 73: 997-1003.

Dalby KN, Morrice N, Caudwell FB, Avruch J, Cohen P (1998): Identification of regulatory phosphorylation sites in mitogen-activated protein kinase (MAPK)-activated protein kinase-1a/p90rsk that are inducible by MAPK. J. Biol. Chem. 273:1496-1505.

Davydenko O, Schultz RM, Lampson MA (2013): Increased CDK1 activity determines the timing of kinetochore-microtubule attachments in meiosis I. J. Cell Biol. 202: 221-229.

** Desai N, Ludgin J, Sharma R, Anirudh RK, Agarwal A (2013): Female and male gametogenesis. *In*: Falcone T, Hurd WW (eds.): Clinical Reproductive Medicine and Surgery. Springer, New York-Heidelberg-Dordrecht-London, 43-62.

Dickson KS, Bilger A, Ballantyne S, Wickens MP (1999): The cleavage and polyadenylation specificity factor in Xenopus laevis oocytes is a cytoplasmic factor involved in regulated polyadenylation. Mol. Cell Biol. 19: 5707-5717.

Ellederova Z, Cais O, Susor A, Uhlirova K, Kovarova H, Jelinkova L, Tomek W, Kubelka M (2008): ERK1/2 map kinase metabolic pathway is responsible for phosphorylation of translation initiation factor eIF4E during in vitro maturation of pig oocytes. Mol. Reprod. Dev. 75: 309-317.

Erickson AK, Payne DM, Martino PA, Rossomando AJ, Shabanowitz J, Weber MJ, Hunt DF, Sturgill TW (1990): Identification by mass spectrometry of threonine 97 in bovine myelin basic protein as a specific phosphorylation site for mitogen-activated protein kinase. J. Biol. Chem. 265: 19728-19735.

Evsikov AV, Graber JH, Brockman JM, Hampl A, Holbrook AE, Singh P, Eppig JJ, Solter D, Knowles BB (2006): Cracking the egg: molecular dynamics and evolutionary aspects of the transition from the fully grown oocyte to embryo. Genes Dev. 20: 2713-2727.

* Fan HY, Sun QY (2004): Involvement of mitogen-activated protein kinase cascade during oocyte maturation and fertilization in mammals. Biol. Reprod. 70: 535-547.

Fox CA, Sheets MD, Wickens MP (1989): Poly(A) addition during maturation of frog oocytes: distinct nuclear and cytoplasmic activities and regulation by the sequence UUUUUAU. Genes Dev. 3: 2151-2162.

Fulka J Jr., Motlik J, Fulka J, Jilek F (1986): Effect of cycloheximide on nuclear maturation of pig and mouse oocytes. J. Reprod. Fertil. 77: 281-285.

Gavin AC, Cavadore JC, Schorderet-Slatkine S (1994): Histone H1 kinase activity, germinal vesicle breakdown and M phase entry in mouse oocytes. J. Cell Sci. 107: 275-283.

Gebauer F, Richter JD (1996): Mouse cytoplasmic polyadenylylation element binding protein: an evolutionarily conserved protein that interacts with the cytoplasmic polyadenylylation elements of c-mos mRNA. Proc. Natl. Acad. Sci. U. S. A. 93: 14602-14607.

Gebauer S, Xu W, Cooper GM, Richter JD (1994): Translational control by cytoplasmic polyadenylation of c-mos mRNA is necessary for oocyte maturation in the mouse. EMBO J. 13: 5712-5720.

* Georges A, Auguste A, Bessiere L, Vanet A, Todeschini AL, Veitia RA (2014): FOXL2: a central transcription factor of the ovary. J. Mol. Endocrinol. 52: R17-33.

Giangarrà V, Igea A, Castellazzi CL, Bava FA, Mendez R (2015): Global Analysis of CPEBs Reveals Sequential and Non-Redundant Functions in Mitotic Cell Cycle. PLoS One. 10: e0138794.

Guzeloglu-Kayisli O, Lalioti MD, Aydiner F, Sasson I, Ilbay O, Sakkas D, Lowther KM, Mehlmann LM, Seli E (2012): Embryonic poly(A)-binding protein (EPAB) is required for oocyte maturation and female fertility in mice. Biochem. J. 446: 47-58.

Hake LE, Mendez R, Richter JD (1998): Specificity of RNA binding by CPEB: requirement for RNA recognition motifs and a novel zinc finger. Mol. Cell Biol. 18: 685-693.

Hake LE, Richter JD (1994): CPEB is a specificity factor that mediates cytoplasmic polyadenylation during Xenopus oocyte maturation. Cell. 79: 617-627.

Hampl A, Eppig JJ (1995a): Analysis of the mechanism(s) of metaphase I arrest in maturing mouse oocytes. Development. 121: 925-933.

Hampl A, Eppig JJ (1995b): Translational regulation of the gradual increase in histone H1 kinase activity in maturing mouse oocytes. Mol. Reprod. Dev. 40: 9-15.

Hao Z, Stoler MH, Sen B, Shore A, Westbrook A, Flickinger CJ, Herr JC, Coonrod SA (2002): TACC3 expression and localization in the murine egg and ovary. Mol. Reprod. Dev. 63: 291-299.

Hara M, Abe Y, Tanaka T, Yamamoto T, Okumura E, Kishimoto T (2012): Greatwall kinase and cyclin B-Cdk1 are both critical constituents of M-phase-promoting factor. Nat. Commun. 3: 1059-1067.

Hashimoto N (1996): Role of c-mos proto-oncogene product in the regulation of mouse oocyte maturation. Horm. Res. 46: 11-14.

Hodgman R, Tay J, Mendez R, Richter JD (2001): CPEB phosphorylation and cytoplasmic polyadenylation are catalyzed by the kinase IAK1/Eg2 in maturing mouse oocytes. Development. 128: 2815-2822.

Huarte J, Stutz A, O'Connell ML, Gubler P, Belin D, Darrow AL, Strickland S, Vassalli JD (1992): Transient translational silencing by reversible mRNA deadenylation. Cell. 69: 1021-1030.

Igea A, Méndez R (2010): Meiosis requires a translational positive loop where CPEB1 ensues its replacement by CPEB4. EMBO J. 29: 2182-2193.

Inoue M, Naito K, Aoki F, Toyoda Y, Sato E (1995): Activation of mitogen-activated protein kinase during meiotic maturation in porcine oocytes. Zygote. 3: 265-271.

* Ivshina M, Lasko P, Richter JD (2014): Cytoplasmic polyadenylation element binding proteins in development, health, and disease. Annu. Rev. Cell Dev. Biol. 30: 393-415.

Jansova D, Koncicka M, Tetkova A, Cerna R, Malik R, Del Llano E, Kubelka M, Susor A (2017): Regulation of 4E-BP1 activity in the mammalian oocyte. Cell Cycle. 8.

Kanatsu-Shinohara M, Schultz RM, Kopf GS (2000): Acquisition of meiotic competence in mouse oocytes: absolute amounts of p34(cdc2), cyclin B1, cdc25C, and wee1 in meiotically incompetent and competent oocytes. Biol. Reprod. 63: 1610-1616.

Keady BT, Kuo P, Martínez SE, Yuan L, Hake LE (2007): MAPK interacts with XGef and is required for CPEB activation during meiosis in Xenopus oocytes. J. Cell Sci. 120: 1093-1103.

Kim JH, Richter JD (2006): Opposing polymerase-deadenylase activities regulate cytoplasmic polyadenylation. Mol. Cell. 24: 173-183.

Kim JH, Richter JD (2007): RINGO/cdk1 and CPEB mediate poly(A) tail stabilization and translational regulation by ePAB. Genes Dev. 21: 2571-2579.

Komrskova P, Susor A, Malik R, Prochazkova B, Liskova L, Supolikova J, Hladky S, Kubelka M (2014): Aurora kinase A is not involved in CPEB1 phosphorylation and cyclin B1 mRNA polyadenylation during meiotic maturation of porcine oocytes. PLoS One. 9: e101222.

Kong BY, Bernhardt ML, Kim AM, O'Halloran TV, Woodruff TK (2012): Zinc maintains prophase I arrest in mouse oocytes through regulation of the MOS-MAPK pathway. Biol. Reprod. 87: 1-12.

Kotani T, Yasuda K, Ota R, Yamashita M (2013): Cyclin B1 mRNA translation is temporally controlled through formation and disassembly of RNA granules. J. Cell Biol. 202: 1041-1055.

Kubiak JZ, Weber M, Geraud G, Maro B (1992): Cell cycle modification during the transitions between meiotic M-phases in mouse oocytes. J. Cell Sci. 102: 457-467.

Kume S, Endo T, Nishimura Y, Kano K, Naito K (2007): Porcine SPDYA2 (RINGO A2) stimulates CDC2 activity and accelerates meiotic maturation of porcine oocytes. Biol. Reprod. 76: 440-447.

Kuo P, Runge E, Lu X, Hake LE (2011): XGef influences XRINGO/CDK1 signaling and CPEB activation during Xenopus oocyte maturation. Differentiation. 81: 133-140.

Laemmli UK (1970): Cleavage of structural proteins during the assembly of the head of bacteriophage T4. Nature. 227: 680-685.

Langan TA, Gautier J, Lohka M, Hollingsworth R, Moreno S, Nurse P, Maller J, Sclafani RA (1989): Mammalian growth-associated H1 histone kinase: a homolog of cdc2+/CDC28 protein kinases controlling mitotic entry in yeast and frog cells. Mol. Cell Biol. 9: 3860-3868.

Lantz V, Ambrosio L, Schedl P (1992): The Drosophila orb gene is predicted to encode sex-specific germline RNA-binding proteins and has localized transcripts in ovaries and early embryos. Development. 115: 75-88.

Lee J, Miyano T, Moor RM (2000): Localisation of phosphorylated MAP kinase during the transition from meiosis I to meiosis II in pig oocytes. Zygote. 8: 119-125.

Lefebvre C, Terret ME, Djiane A, Rassinier P, Maro B, Verlhac MH (2002): Meiotic spindle stability depends on MAPK-interacting and spindle-stabilizing protein (MISS), a new MAPK substrate. J. Cell Biol. 157: 603-613.

Leonardsen L, Wiersma A, Baltsen M, Byskov AG, Andersen CY (2000): Regulation of spontaneous and induced resumption of meiosis in mouse oocytes by different intracellular pathways. J. Reprod. Fertil. 120: 377-383.

Lincoln AJ, Wickramasinghe D, Stein P, Schultz RM, Palko ME, De Miguel MP, Tessarollo L, Donovan PJ (2002): Cdc25b phosphatase is required for resumption of meiosis during oocyte maturation. Nat. Genet. 30: 446-449.

Liu H, Gao Y, Zhai B, Jiang H, Ding Y, Zhang L, Li C, Deng Q, Yu X, Zhang J (2016): The Effects of Polyadenylation Status on MPFs During In Vitro Porcine Oocyte Maturation. Cell Physiol. Biochem. 39: 1735-1745.

Masui Y, Markert CL (1971): Cytoplasmic control of nuclear behavior during meiotic maturation of frog oocytes. J. Exp. Zool. 177: 129-145.

McGrew LL, Dworkin-Rastl E, Dworkin MB, Richter JD (1989): Poly(A) elongation during Xenopus oocyte maturation is required for translational recruitment and is mediated by a short sequence element. Genes Dev. 3: 803-815.

Mendez R1, Barnard D, Richter JD (2002): Differential mRNA translation and meiotic progression require Cdc2-mediated CPEB destruction. EMBO J. 21: 1833-1844.

Mendez R, Hake LE, Andresson T, Littlepage LE, Ruderman JV, Richter JD (2000a): Phosphorylation of CPE binding factor by Eg2 regulates translation of c-mos mRNA. Nature. 404: 302-307.

Mendez R, Murthy KG, Ryan K, Manley JL, Richter JD (2000b): Phosphorylation of CPEB by Eg2 mediates the recruitment of CPSF into an active cytoplasmic polyadenylation complex. Mol. Cell. 6:1253-1259.

Minshall N, Reiter MH, Weil D, Standart N (2007): CPEB interacts with an ovary-specific eIF4E and 4E-T in early Xenopus oocytes. J. Biol. Chem. 282: 37389-37401.

Motlík J, Sutovský P, Kalous J, Kubelka M, Moos J, Schultz RM (1996): Co-culture with pig membrana granulosa cells modulates the activity of cdc2 and MAP kinase in maturing cattle oocytes. Zygote. 4: 247-256.

Nishimura Y, Kano K, Naito K (2010): Porcine CPEB1 is involved in Cyclin B translation and meiotic resumption in porcine oocytes. Anim. Sci. J. 81: 444-452.

* Nurse P (1990): Universal control mechanism regulating onset of M-phase. Nature. 344: 503-508.

Oh JS, Han SJ, Conti M (2010): Wee1B, Myt1, and Cdc25 function in distinct compartments of the mouse oocyte to control meiotic resumption. J. Cell Biol. 188: 199-207.

Paules RS, Buccione R, Moschel RC, Vande Woude GF, Eppig JJ (1989): Mouse Mos protooncogene product is present and functions during oogenesis. Proc. Natl. Acad. Sci. U. S. A. 86: 5395-5399.

Pearson RB, Kemp BE (1991): Protein kinase phosphorylation site sequences and consensus specificity motifs: tabulations. Methods Enzymol. 200: 62-81.

Piqué M, López JM, Foissac S, Guigó R, Méndez R (2008): A combinatorial code for CPE-mediated translational control. Cell. 132: 434-448.

Racki WJ, Richter JD (2006): CPEB controls oocyte growth and follicle development in the mouse. Development. 133: 4527-4537.

* Rissland OS (2017): The organization and regulation of mRNA-protein complexes. Wiley Interdiscip. Rev.: RNA. 8: 1-17.

* Roskoski R Jr. (2012): ERK1/2 MAP kinases: structure, function, and regulation. Pharmacol. Res. 66: 105-143.

Salles FJ, Strickland S (1995): Rapid and sensitive analysis of mRNA polyadenylation states by PCR. PCR Methods Appl. 4: 317-321.

Sarkissian M, Mendez R, Richter JD (2004): Progesterone and insulin stimulation of CPEB-dependent polyadenylation is regulated by Aurora A and glycogen synthase kinase-3. Genes Dev. 18: 48-61.

Sha QQ, Dai XX, Dang Y, Tang F, Liu J, Zhang YL, Fan HY (2016): A MAPK cascade couples maternal mRNA translation and degradation to meiotic cell cycle progression in mouse oocytes. Development. 144: 452-463.

Shimaoka T, Nishimura T, Kano K, Naito K (2009): Critical effect of pigWee1B on the regulation of meiotic resumption in porcine immature oocytes. Cell Cycle. 8: 2375-2384.

** Somfai T, Hirao Y (2011): Synchronization of in vitro maturation in porcine oocytes. *In*: Banfalvi G (ed.): Cell Cycle Synchronization. Springer, New York-Heidelberg-Dordrecht-London, 211-225.

Stebbins-Boaz B, Cao Q, de Moor CH, Mendez R, Richter JD (1999): Maskin is a CPEB-associated factor that transiently interacts with eIF-4E. Mol. Cell. 4: 1017-1027.

Su YQ, Eppig JJ (2002): Evidence that multifunctional calcium/calmodulin-dependent protein kinase II (CaM KII) participates in the meiotic maturation of mouse oocytes. Mol. Reprod. Dev. 61: 560-569.

Su YQ, Rubinstein S, Luria A, Lax Y, Breitbart H (2001): Involvement of MEK-mitogen-activated protein kinase pathway in follicle-stimulating hormone-induced but not spontaneous meiotic resumption of mouse oocytes. Biol. Reprod. 65: 358-365.

Susor A, Jansova D, Cerna R, Danylevska A, Anger M, Toralova T, Malik R, Supolikova J, Cook MS, Oh JS, Kubelka M (2015): Temporal and spatial regulation of translation in the mammalian oocyte via the mTOR-eIF4F pathway. Nat. Commun. 6: 6078.

Tay J, Hodgman R, Richter JD (2000): The control of cyclin B1 mRNA translation during mouse oocyte maturation. Dev. Biol. 221: 1-9.

Tay J, Richter JD (2001): Germ cell differentiation and synaptonemal complex formation are disrupted in CPEB knockout mice. Dev. Cell. 1: 201-213.

Terret ME, Lefebvre C, Djiane A, Rassinier P, Moreau J, Maro B, Verlhac MH (2003): DOC1R: a MAP kinase substrate that control microtubule organization of metaphase II mouse oocytes. Development. 130: 5169-5177.

Tong C, Fan HY, Chen DY, Song XF, Schatten H, Sun QY (2003): Effects of MEK inhibitor U0126 on meiotic progression in mouse oocytes: microtuble organization, asymmetric division and metaphase II arrest. Cell Res. 13: 375-383.

Uzbekova S, Arlot-Bonnemains Y, Dupont J, Dalbiès-Tran R, Papillier P, Pennetier S, Thélie A, Perreau C, Mermillod P, Prigent C, Uzbekov R (2008): Spatio-temporal expression patterns of aurora kinases a, B, and C and cytoplasmic polyadenylation-element-binding protein in bovine oocytes during meiotic maturation. Biol. Reprod. 78: 218-233.

* Van den Hurk R, Zhao J (2005): Formation of mammalian oocytes and their growth, differentiation and maturation within ovarian follicles. Theriogenology. 63: 1717-1751.

Verlhac MH, de Pennart H, Maro B, Cobb MH, Clarke HJ (1993): MAP kinase becomes stably activated at metaphase and is associated with microtubule-organizing centers during meiotic maturation of mouse oocytes. Dev. Biol. 158: 330-340.

Verlhac MH, Kubiak JZ, Clarke HJ, Maro B (1994): Microtubule and chromatin behavior follow MAP kinase activity but not MPF activity during meiosis in mouse oocytes. Development. 120: 1017-1025.

Verlhac MH, Kubiak JZ, Weber M, Geraud G, Colledge WH, Evans MJ, Maro B (1996): Mos is required for MAP kinase activation and is involved in microtubule organization during meiotic maturation in the mouse. Development. 122: 815-822.

Verlhac MH, Lefebvre C, Kubiak JZ, Umbhauer M, Rassinier P, Colledge WH, Maro B (2000): Mos activates MAP kinase in mouse oocytes through two opposite pathways. EMBO J. 19: 6065-6074.

Villaescusa JC, Allard P, Carminati E, Kontogiannea M, Talarico D, Blasi F, Farookhi R, Verrotti AC (2006): Clast4, the murine homologue of human eIF4E-Transporter, is highly expressed in developing oocytes and post-translationally modified at meiotic maturation. Gene. 367: 101-109.

* Wek RC, Jiang HY, Anthony TG (2006): Coping with stress: eIF2 kinases and translational control. Biochem. Soc. Trans. 34: 7-11.

Welk JF, Charlesworth A, Smith GD, MacNicol AM (2001): Identification and characterization of the gene encoding human cytoplasmic polyadenylation element binding protein. Gene. 263: 113-120.

Wilson R, Ainscough R, Anderson K, Baynes C, Berks M, Bonfield J, Burton J, Connell M, Copsey T, Cooper J, *et al*. (1994): 2.2 Mb of contiguous nucleotide sequence from chromosome III of C. elegans. Nature. 368: 32-38.

Wongsrikeao P, Kaneshige Y, Ooki R, Taniguchi M, Agung B, Nii M, Otoi T (2005): Effect of the removal of cumulus cells on the nuclear maturation, fertilization and development of porcine oocytes. Reprod. Domest. Anim. 40: 166-170.

Yang CR, Wei Y, Qi ST, Chen L, Zhang QH, Ma JY, Luo YB, Wang YP, Hou Y, Schatten H, Liu ZH, Sun QY (2012): The G protein coupled receptor 3 is involved in cAMP and cGMP signaling and maintenance of meiotic arrest in porcine oocytes. PLoS One. 7: e38807.

Yang Q, Allard P, Huang M, Zhang W, Clarke HJ (2010): Proteasomal activity is required to initiate and to sustain translational activation of messenger RNA encoding the stem-loop-binding protein during meiotic maturation in mice. Biol. Reprod. 82: 123-131.

Ye J, Flint AP, Luck MR, Campbell KH (2003): Independent activation of MAP kinase and MPF during the initiation of meiotic maturation in pig oocytes. Reproduction. 125: 645-656.

Yu C, Ji SY, Sha QQ, Dang Y, Zhou JJ, Zhang YL, Liu Y, Wang ZW, Hu B, Sun QY, Sun SC, Tang F, Fan HY (2016): BTG4 is a meiotic cell cycle-coupled maternal-zygotic-transition licensing factor in oocytes. Nat. Struct. Mol. Biol. 23: 387-394.

Zhang DX, Cui XS, Kim NH (2010a): Molecular characterization and polyadenylation-regulated expression of cyclin B1 and Cdc2 in porcine oocytes and early parthenotes. Mol. Reprod. Dev. 77: 38-50.

Zhang X, Miao Y, Zhao JG, Spate L, Bennett MW, Murphy CN, Schatten H, Prather RS (2010b): Porcine oocytes denuded before maturation can develop to the blastocyst stage if provided a cumulous cell-derived coculture system. J. Anim. Sci. 88: 2604-2610.

Zhang YL, Liu XM, Ji SY, Sha QQ, Zhang J, Fan HY (2015): ERK1/2 activities are dispensable for oocyte growth but are required for meiotic maturation and pronuclear formation in mouse. J. Genet. Genomics. 42: 477-485.

SUPPLEMENTARY INFORMATION

Fig. S1. Sequence of 3'UTR of mouse cyclin B1 mRNA

3'UTR of mouse cyclin B1 mRNA contains four polyadenylation signals (PAS1-4, red rectangles) and four CPE-like sequences (CPE, blue rectangles). The forward primer used for poly(A) tail assay is labeled by black arrow. Using this primer, polyadenylation of the cyclin B1 transcript generated by cleavage of cyclin B1 pre-mRNA just downstream of PAS4 is assessed. STOP, stop codon.

Fig. S2. Sequence of part of coding region and 3'UTR of porcine cyclin B1 mRNA

3'UTR of porcine cyclin B1 mRNA contains three polyadenylation signals (PAS1-3, red rectangles) and five CPE-like sequences (CPE, blue rectangles). The forward primer used for poly(A) tail assay is labeled by black arrow. Using this primer, polyadenylation of both long and short cyclin B1 transcript isoforms is assessed. The long and short isoforms are generated by cleavage of cyclin B1 pre-mRNA just downstream of PAS3 and PAS2, respectively. STOP, stop codon.